Heterodimerization of serotonin receptors 5-HT$_{1A}$ and 5-HT$_7$ differentially regulates receptor signalling and trafficking

Ute Renner[1,*], Andre Zeug[1,2,*], Andrew Woehler[2,3], Marcus Niebert[2], Alexander Dityatev[4], Galina Dityateva[4], Nataliya Gorinski[1], Daria Guseva[1], Dalia Abdel-Galil[1], Matthias Fröhlich[5], Frank Döring[5], Erhard Wischmeyer[5], Diethelm W. Richter[2], Erwin Neher[2,3] and Evgeni G. Ponimaskin[1,2,‡]

[1]DFG-Research Center Molecular Physiology of the Brain (CMPB), 37077 Göttingen, Germany
[2]Cellular Neurophysiology, Center of Physiology, Medical School Hannover, Carl-Neuberg Strasse, 30625 Hannover, Germany
[3]Max-Plank-Institute for Biophysical Chemistry, 37077 Göttingen, Germany
[4]Department of Neuroscience and Brain Technologies, Italian Institute of Technology, 16163 Genova, Italy
[5]Institute for Physiology, University of Würzburg, 97070 Würzburg, Germany

*These authors contributed equally to this work
‡Author for correspondence (ponimaskin.evgeni@mh-hannover.de)

Accepted 11 January 2012
Journal of Cell Science 125, 2486–2499

doi: 10.1242/jcs.101337

Summary

Serotonin receptors 5-HT$_{1A}$ and 5-HT$_7$ are highly coexpressed in brain regions implicated in depression. However, their functional interaction has not been established. In the present study we show that 5-HT$_{1A}$ and 5-HT$_7$ receptors form heterodimers both in vitro and in vivo. Foerster resonance energy transfer-based assays revealed that, in addition to heterodimers, homodimers composed either of 5-HT$_{1A}$ or 5-HT$_7$ receptors together with monomers coexist in cells. The highest affinity for complex formation was obtained for the 5-HT$_7$–5-HT$_7$ homodimers, followed by the 5-HT$_7$–5-HT$_{1A}$ heterodimers and 5-HT$_{1A}$–5-HT$_{1A}$ homodimers. Functionally, heterodimerization decreases 5-HT$_{1A}$-receptor-mediated activation of G_i protein without affecting 5-HT$_7$-receptor-mediated signalling. Moreover, heterodimerization markedly decreases the ability of the 5-HT$_{1A}$ receptor to activate G-protein-gated inwardly rectifying potassium channels in a heterologous system. The inhibitory effect on such channels was also preserved in hippocampal neurons, demonstrating a physiological relevance of heteromerization in vivo. In addition, heterodimerization is crucially involved in initiation of the serotonin-mediated 5-HT$_{1A}$ receptor internalization and also enhances the ability of the 5-HT$_{1A}$ receptor to activate the mitogen-activated protein kinases. Finally, we found that production of 5-HT$_7$ receptors in the hippocampus continuously decreases during postnatal development, indicating that the relative concentration of 5-HT$_{1A}$–5-HT$_7$ heterodimers and, consequently, their functional importance undergoes pronounced developmental changes.

Key words: G-protein coupled receptor, Oligomerization, Signal transduction

Introduction

G-protein-coupled receptors (GPCRs) belong to a large and diverse family of integral membrane proteins that participate in the regulation of many cellular processes and, therefore, represent key targets for pharmacological treatment. Until recently, GPCRs were assumed to exist and function as monomeric units that interact with corresponding G proteins in a 1:1 stoichiometry. However, biochemical, structural and functional evidence collected during the last decade indicates that GPCRs can form oligomers (Devi, 2001; Bulenger et al., 2005).

Oligomerization can occur between identical receptor types (homomerization) or between different receptors of the same or different GPCR families (heteromerization). Heteromerization is of particular interest because it can specifically modulate receptor properties. It can lead to significant changes in receptor pharmacology, either by affecting the ligand binding on individual protomers or by the formation of new binding sites (Franco, 2009; Rozenfeld and Devi, 2011). Accumulating evidence also indicates that heteromerization might affect signalling pathways regulated by a given protomer. For example, a synergistic increase of the receptor-mediated signalling was observed for the adrenergic α_{1A}AR–α_{1B}AR and the muscarinic M_2R–M_3R heterodimers (Hornigold et al., 2003; Israilova et al., 2004; Fuxe et al., 2005). On the other hand, G protein signalling might be attenuated upon heteromerization, as has been reported for the opiate MOR–DOR, the α_{2A}AR–MOR and the adenosine–dopamine A_{2A}R–D_2R heterodimers (Gomes et al., 2000; Jordan et al., 2003). Moreover, heteromerization can lead to a switch in G protein coupling, as previously shown for dopamine D_1R–D_2R heteromers (Lee et al., 2004). Thus, heteromerization might provide an additional level of control for the regulation of cellular processes by fine tuning of receptor-mediated signalling.

In the present study, we examined the heteromerization of two members of the serotonin receptor family, 5-HT$_{1A}$ and 5-HT$_7$ receptors. The 5-HT$_{1A}$ receptor is coupled to members of the $G_{i/o}$ protein family, which induce inhibition of adenylyl cyclase and subsequent decrease of intracellular cAMP levels (Barnes and Sharp, 1999; Raymond et al., 1999; Pucadyil et al., 2005). In addition, stimulation of 5-HT$_{1A}$ receptors leads to a Gβγ-mediated activation of K^+ channels as well as to activation of the mitogen-activated protein (MAP) kinase Erk2 (Fargin et al., 1989; Garnovskaya et al., 1996). With respect to physiological

functions, considerable interest in the 5-HT$_{1A}$ receptor has been raised due to its involvement in depression and anxiety states (Parks et al., 1998; Gordon and Hen, 2004).

The 5-HT$_7$ receptor is one of the most recently described members of the 5-HT receptor family (Barnes and Sharp, 1999; Hedlund and Sutcliffe, 2004). The 5-HT$_7$ receptor stimulates cAMP formation by activating adenylyl cyclases via the G_s proteins (Norum et al., 2003). This receptor is associated with a number of physiological and pathophysiological responses, including serotonin-induced phase shifting of the circadian rhythm (Lovenberg et al., 1993) and age-dependent changes in the circadian timing (Duncan et al., 1999). In addition, a large body of evidence indicates an involvement of the 5-HT$_7$ receptor in the development of anxiety and depression, and recent studies have shown that the 5-HT$_7$ receptor is most probably clinically relevant for the treatment of depression (Hedlund, 2009).

Recently, we have demonstrated that 5-HT$_{1A}$ receptors form homodimers at the plasma membrane (Kobe et al., 2008; Woehler et al., 2009). Formation of 5-HT$_{1A}$ homomers (including the higher-order oligomers) was further confirmed by several more recent publications (Ganguly et al., 2011; Paila et al., 2011). Here, we report that 5-HT$_{1A}$ receptors can form heterodimers with 5-HT$_7$ receptors both in vitro as well as in vivo. In addition, we propose a dynamic dimerization model that allows calculation of relative concentrations of monomers, homo- and heterodimers as a function of receptor expression level. We also demonstrate that heterodimerization decreases G_i protein coupling of the 5-HT$_{1A}$ receptor and attenuates receptor-mediated activation of potassium channels without substantial changes in the coupling of the 5-HT$_7$ receptor to the G_s protein. Moreover, heterodimerization significantly facilitates internalization of the 5-HT$_{1A}$ receptor as well as its ability to activate MAP kinase.

Results

5-HT$_{1A}$ and 5-HT$_7$ receptors form heterodimers

Specific interaction between 5-HT$_{1A}$ and 5-HT$_7$ receptors was analysed by co-immunoprecipitation experiments in N1E-115 cells coexpressing haemagglutinin (HA)- and YFP-tagged receptors. Fig. 1A shows that after immunoprecipitation with an antibody against the HA-tag, YFP-tagged receptors were identified only in samples derived from cells coexpressing both HA- and YFP-tagged receptors. To assay the extent of artificial protein aggregation, cells expressing only one type of receptor (HA- or YFP-tagged) were mixed prior to lysis and analysed in parallel. As shown in Fig. 1A, individual receptors can be detected by the same antibody, but co-immunoprecipitation did not occur. This further verifies the specificity of 5-HT$_{1A}$–5-HT$_7$ hetero-oligomerization.

We then examined Förster resonance energy transfer (FRET) occurrence between fluorophore-labelled 5-HT$_{1A}$ and 5-HT$_7$ receptors in living neuroblastoma cells. To avoid artefacts resulting from overexpression, we adjusted the receptor expression to 1.000–1.200 fmol/mg protein, which is similar to the endogenous expression level in vivo (Pazos and Palacios, 1985; Hoyer et al., 1986; Kobe et al., 2008). Fig. 1B shows the typical fluorescence emission spectra at 420 nm excitation obtained in suspensions of cells expressing 5-HT$_{1A}$–CFP, 5-HT$_7$–YFP or coexpressing 5-HT$_{1A}$–CFP and 5-HT$_7$–YFP as a FRET pair. When cells were transfected with only CFP-fused receptor, the typical emission spectrum of CFP was obtained with emission peaks at 475 nm and 500 nm (Fig. 1B). The emission spectrum obtained from cells expressing only the YFP-fused receptor showed a very weak peak at 525 nm. By contrast, cells coexpressing 5-HT$_{1A}$–CFP and 5-HT$_7$–YFP receptors demonstrated a significantly larger emission peak at 525 nm concomitant with a smaller CFP emission, which demonstrates the energy transfer from CFP to YFP (Fig. 1B) and confirms the 5-HT$_{1A}$–5-HT$_7$ heterodimerization in living cells. To analyse the effect of agonist stimulation on receptor oligomerization, we measured the FRET efficiency in suspensions of cells co-transfected with donor (5-HT$_{1A}$–CFP) and acceptor (5-HT$_7$–YFP) proteins at a 1:1 ratio during receptor stimulation with serotonin. Fig. 1C demonstrates that the time course of FRET obtained upon 5-HT treatment was indistinguishable from that in cells treated with phosphate-buffered saline (PBS), demonstrating that the oligomerization state of 5-HT$_{1A}$–5-HT$_7$ complexes is not modulated by the agonist.

Analysis of receptor heteromerization by acceptor photobleaching FRET

A microscope-based acceptor photobleaching FRET assay (Kobe et al., 2008) was applied to study 5-HT$_{1A}$–5-HT$_7$ heterodimerization at the subcellular level. CFP- and YFP-tagged receptors were expressed in N1E-115 cells, and the plasma membrane localized receptors were targeted for acceptor photobleaching analysis (Fig. 2A). Fig. 2B,C illustrates changes in emission intensities of donor and acceptor fluorescence in the bleached and non-bleached regions of interest, demonstrating that a loss of acceptor fluorescence was accompanied by an increase of donor emission intensity, which is characteristic for FRET. For cells expressing fluorescence-tagged 5-HT$_{1A}$ receptors with similar donor (CFP) to acceptor (YFP) ratios, a mean apparent FRET efficiency of 20±1% (n=24) was measured (Fig. 2D), which is in accordance with our previous results (Kobe et al., 2008). Similar FRET values were obtained for 5-HT$_7$ homodimers, with a mean apparent FRET efficiency of 21±2% (n=20) (Fig. 2D). In the case of coexpression of 5-HT$_7$–CFP (donor) and 5-HT$_{1A}$–YFP (acceptor) as a FRET pair, the apparent FRET efficiency was 20±2% (n=21) (Fig. 2D), and this value was not significantly different when 5-HT$_{1A}$–CFP was used as a donor and 5-HT$_7$–YFP as an acceptor (Ef_D=23±2%, n=22). As a negative control, we used co-transfection of 5-HT$_7$–CFP receptor and non-relevant transmembrane protein CD86–YFP. This protein is known to be a monomer and, therefore, it is often used as a negative control in methods that study protein–protein interaction by resonance energy transfer (James et al., 2006; Dorsch et al., 2009). In accordance with published data, in such negative control experiments we found significantly reduced, but still not zero, apparent FRET values (11±1% n=22; Fig. 2D). The main reason for such observation is an enriched local concentration of CD86–YFP and 5-HT7–CFP (which both are transmembrane proteins) at the plasma membrane after co-transfection, which results in nonspecific donor–acceptor interactions. Significantly lower FRET efficiency was also obtained after the co-transfection of CD86–YFP with 5-HT$_{1A}$–CFP and of CD86–YFP with CD86–CFP (data not shown). These results indicate that 5-HT$_{1A}$ and 5-HT$_7$ receptors can form both homo- and heterodimers at the cell surface.

Relative amounts of homo- and heterodimers depend on the expression ratio between 5-HT$_{1A}$ and 5-HT$_7$ receptor

Results of the acceptor photobleaching FRET experiments demonstrated the existence of three principal kinds of oligomers after receptor coexpression, which includes two types of homodimer (5-HT$_{1A}$–5-HT$_{1A}$ and 5-HT$_7$–5-HT$_7$) as

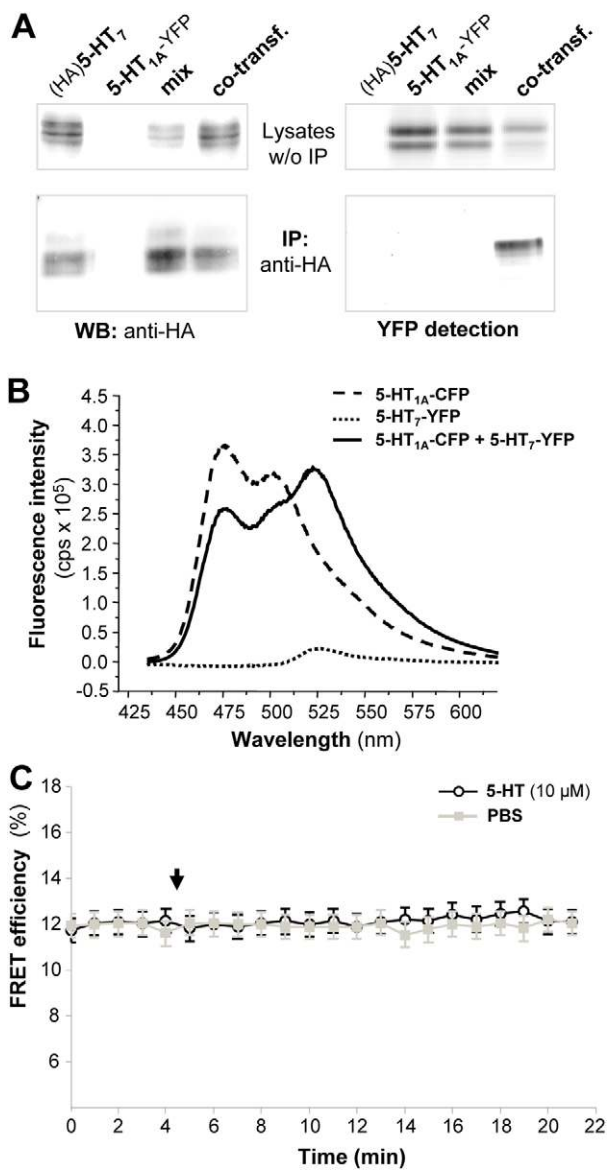

Fig. 1. Analysis of 5-HT$_{1A}$–5-HT$_7$ receptor heterodimerization. (**A**) Specific interactions between recombinant HA-tagged 5-HT$_7$ and YFP-tagged 5-HT$_{1A}$ receptors. Neuroblastoma N1E-115 cells coexpressing HA- and YFP-tagged receptors (co-transf.), a mixture of cells expressing each receptor individually (mix) or single-transfected cells were subjected to SDS-PAGE (10%) followed by western blot (on the left) or fluorescence detection (on the right). The results before (upper panel) and after (lower panel) immunoprecipitation are shown. IP refers to the antibodies used for immunoprecipitation, and WB defines the antibody used for immunoblotting. The results shown are representative of at least four independent experiments. (**B**) Spectral analysis of N1E-115 cells coexpressing CFP- and YFP-tagged 5-HT$_{1A}$ and 5-HT$_7$ receptors, respectively. Fluorescence emission spectra of living N1E-115 cells transfected with either 5-HT$_{1A}$–CFP (dashed line) or 5-HT$_7$–YFP (dotted line) receptors, or co-transfected with both YFP- and CFP-tagged receptors (solid line) are shown. Emission spectra were collected at excitation wavelength of 420 nm. Spectra were normalized to that obtained in cells transfected with HA-tagged 5-HT$_{1A}$ receptor. The data shown are representative of at least three independent experiments. (**C**) Time course of changes in FRET efficiencies upon receptor stimulation. Suspension of N1E-115 cells coexpressing 5-HT$_{1A}$–CFP and 5-HT$_7$–YFP receptors were treated either with serotonin (10 µm) or PBS. The time-point of treatment is shown by the arrow. Data points represent mean ± s.e.m. (n=4).

well as heterodimer (5-HT$_{1A}$–5-HT$_7$). In addition, a certain number of receptors are expected to be expressed as monomers. To study the oligomerization behaviour of 5-HT$_{1A}$ and 5-HT$_7$ receptors in more detail, we used the quantitative lux-FRET method (Wlodarczyk et al., 2008) to calculate and visualize (Fig. 3B) the apparent FRET efficiencies for donors, Ef_D, and acceptors, Ef_A, over a wide range of donor molar fractions, x_D, where $x_D=[D^t]/([D^t]+[A^t])$, $[D^t]$ is the total donor concentration and $[A^t]$ is the total acceptor concentration. To be able to compare FRET values obtained at different donor to acceptor ratios, the total concentration of plasmids encoding for donor and acceptor was held constant in all experiments. Based on the dependence of both Ef_D and Ef_A on x_D, we first estimated the number of units (n) participating in complex formation (Veatch and Stryer, 1977; Meyer et al., 2006) and obtained a best fit for the value of n=2 (R^2=0.94 and 0.89 for 5-HT$_{1A}$ and 5-HT$_7$ receptors, respectively), demonstrating the preferential formation of dimers (supplementary material Fig. S1). This is also in accordance with our previous results on the 5-HT$_{1A}$ receptor (Kobe et al., 2008; Woehler et al., 2009). Further analysis revealed a linear dependence and symmetry of the apparent FRET efficiencies Ef_D and Ef_A over x_D in the case of 5-HT$_{1A}$ and 5-HT$_7$ homodimers (Fig. 3A). By contrast, coexpression of 5-HT$_{1A}$ and 5-HT$_7$ receptors resulted in highly non-symmetrical distribution of the Ef_D and Ef_A values (Fig. 3A), which cannot be sufficiently fitted (R^2=0.76) by the model suggested by Veatch and Stryer (Veatch and Stryer, 1977). To explain such asymmetry, we developed a general dimerization model describing Ef_D and Ef_A as a function of the total donor and acceptor concentrations (see Materials and Methods for details). The model also considered possible differences in the interaction efficiencies between monomers for the formation of homo- and heterodimers as well as different characteristic FRET efficiencies for the dimer compositions (Fig. 3C; supplementary material Fig. S2). By fitting the model to experimental data we obtained relative dissociation constants in the order of $K_{1A–1A}$=1.05>$K_{1A–7}$=0.27>$K_{7–7}$=0.016 (R^2=0.93; Fig. 3C), where lower K values correspond to a higher tendency to form the particular dimer. For this calculation, the unknown total concentration of receptors (sum of donor and acceptor fluorophores) was assumed to be constant and used as the ‘unit’ concentration. Note that at the relative low, physiologically relevant total receptor concentrations used in the present study, the variability of Ef_D and Ef_A at high x_D values (i.e. high amount of donor and low amount of acceptor) is relative high, because at such conditions the specific YFP fluorescence can hardly be distinguished from cell background. According to these results, the 5-HT$_7$ receptor possesses the highest affinity to form homodimers, followed by the 5-HT$_7$–5-HT$_{1A}$ heterodimers and 5-HT$_{1A}$–5-HT$_{1A}$ homodimers. Using the reaction scheme shown in Fig. 3C, we were also able to predict the relative concentration of monomers and dimers at any given defined expression ratio between 5-HT$_{1A}$ and 5-HT$_7$ receptors. As shown in Fig. 3D, differences in the affinity for forming homo- and heterodimers led to asymmetric distributions of relative concentrations for 5-HT$_{1A}$–5-HT$_{1A}$, 5-HT$_7$–5-HT$_7$ and 5-HT$_{1A}$–5-HT$_7$ dimers as well as the corresponding monomers, when plotted against the expression ratios (see also supplementary material Fig. S3). For instance, an equal amount of homo- and heterodimers can be obtained only at a 5-HT$_{1A}$ to 5-HT$_7$ ratio of 2:1 (x_D value of 0.65), whereas at equal expression levels (1:1 ratio, x_D value of

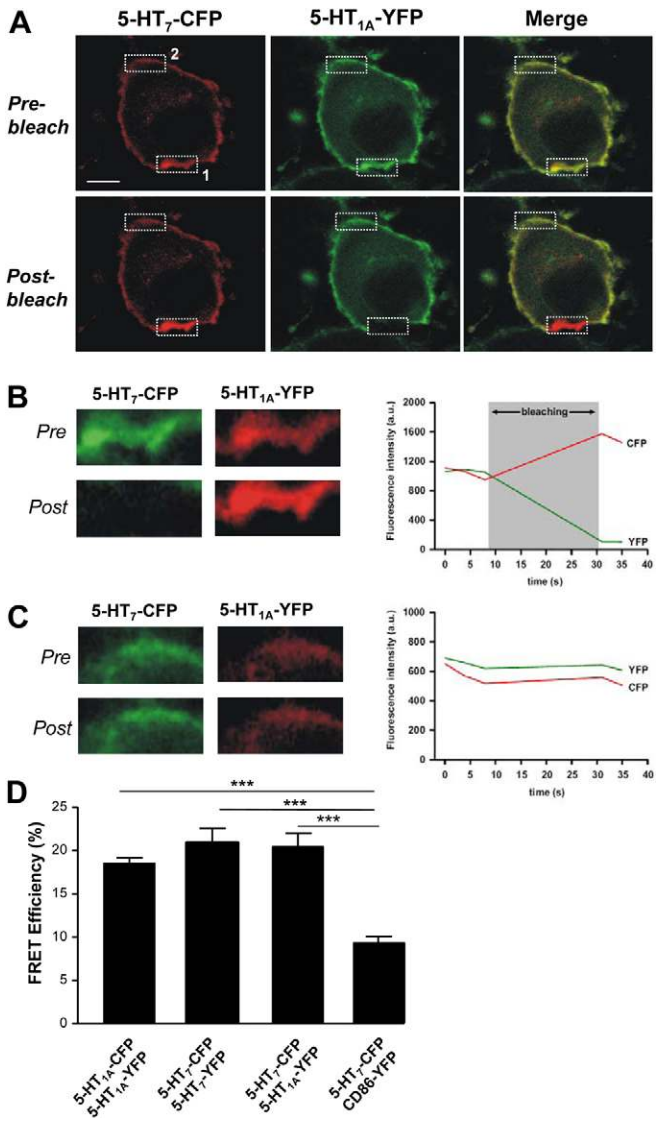

Fig. 2. Acceptor photobleaching FRET analysis of 5-HT$_{1A}$–5-HT$_7$ receptor heteromerization. (**A**) Confocal microscopy was used to visualize 5-HT$_{1A}$–YFP and 5-HT$_7$–CFP receptors coexpressed in the plasma membrane of N1E-115 cells. Fluorescence spectra were collected from a 2 μm optical slice and unmixed to CFP and YFP components using the Zeiss LSM510-Meta detector. The fluorescence image of the CFP channel (green), the YFP channel (red) and composite channel before and after bleaching are shown. Box 1 corresponds to the bleached regions of interest, and box 2 to the non-bleached region of interest. Scale bar: 10 μm. (**B**) Enlargement of box 1 is shown on the left. The 12-bit grayscale intensities of YFP and CFP during the whole trial are plotted for the bleached region of interest (right). (**C**) Enlargement of box 2 is shown on the left. The 12-bit grayscale intensities of YFP and CFP during the whole trial are plotted for the non-bleached region of interest (right). (**D**) Apparent FRET efficiency Ef_D was calculated according to eq. 1 and eq. 2. Bars show mean + s.e.m.; ***P<0.001.

0.5), the relative amount of 5-HT$_7$–5-HT$_{1A}$ heterodimers will be higher than for the 5-HT$_{1A}$ homodimers (Fig. 3D).

Heterodimerization enhances the internalization of 5-HT$_{1A}$ receptors

Next, we examined the consequences of 5-HT$_{1A}$–5-HT$_7$ heterodimerization for the agonist-induced receptor endocytosis by using quantitative analysis of surface-expressed receptors labelled with quantum dots (QDs). Equal labelling of each receptor subtype was assessed by fluorescence-activated cell sorting (FACS) analysis. Serotonin-mediated receptor internalization was then analysed in N1E-115 neuroblastoma cells using total internal reflection fluorescence (TIRF) microscopy by counting the number of QD-labelled puncta visible on the surface during the incubation time (Fig. 4). Analysis of non-stimulated cells revealed that the QDs were stably associated with the plasma membrane and did not change during the incubation period (data not shown). Prolonged stimulation of cells expressing HA-tagged 5-HT$_{1A}$ receptors with serotonin showed no significant receptor internalization, even after 30 minutes of observation (n=4) (Fig. 4A,F,G; supplementary material Movie 1). By contrast, serotonin treatment of N1E cells expressing myc-tagged 5-HT$_7$ receptors resulted in profound internalization of receptors after 11±2 minutes (n=4) (Fig. 4B,F,G; supplementary material Movie 2). To analyse whether heterodimerization can influence receptor internalization, neuroblastoma cells were co-transfected with HA-tagged 5-HT$_{1A}$ and myc-tagged 5-HT$_7$ receptors, and serotonin-mediated re-distribution of QDs bound to the 5-HT$_{1A}$ receptors was studied. As shown in Fig. 4C, 5-HT$_{1A}$–5-HT$_7$ heterodimerization led to pronounced agonist-mediated co-internalization of 5-HT$_{1A}$ receptor (n=4) (Fig. 4C,F,G; supplementary material Movie 3). It is noteworthy that treatment of cells coexpressing 5-HT$_{1A}$ and 5-HT$_7$ receptors with specific 5-HT$_{1A}$ receptor antagonist WAY100635 did not affect serotonin-mediated 5-HT$_{1A}$ receptor internalization (Fig. 4D,F,G). By contrast, pharmacological blockade of 5-HT$_7$ receptor with SB269970 completely abolished agonist-induced 5-HT$_{1A}$ receptor internalization (Fig. 4E,F,G). These results suggest that 5-HT$_7$-receptor-mediated signalling is necessary for initiation of the co-internalization of 5-HT$_{1A}$ receptors.

Finally, we verified that the decreased intensity obtained by the TIRF analysis is indeed caused by the internalization of receptor-bound QDs. After TIRF measurements, all samples were imaged using confocal microscopy followed by 3D-image reconstruction. Such analysis revealed that the loss of QD fluorescence at the cell surface was accompanied by accumulation of fluorescence signal within intracellular compartments (Fig. 5).

Heterodimerization alters signalling properties of the 5-HT$_{1A}$ receptor

The 5-HT$_{1A}$ and 5-HT$_7$ receptors differ in their intracellular signalling in that 5-HT$_{1A}$ is coupled to pertussis-toxin-sensitive members of the $G_{i/o}$ families, whereas the 5-HT$_7$ receptor stimulates adenylyl cyclases via the G_s protein. To determine whether 5-HT$_{1A}$–5-HT$_7$ hetero-dimerization leads to changes in receptor-mediated signalling, we first examined receptor-mediated activation of heteromeric G proteins through a GTPγS coupling assay (Kvachnina et al., 2005). As expected, significant increase in [^{35}S]GTPγS binding to stimulatory Gα$_s$-subunit was measured upon serotonin treatment of cells expressing only the 5-HT$_7$ receptor (Fig. 6A). More importantly, 5-HT$_7$-receptor-mediated activation of G_s protein was not affected by the coexpression of 5-HT$_{1A}$ receptors. By contrast, 5-HT$_{1A}$-receptor-mediated activation of inhibitory G_i protein obtained in cells expressing the 5-HT$_{1A}$ receptors was decreased after coexpression of the 5-HT$_7$ receptor (Fig. 6A). Thus, 5-HT$_{1A}$–5-HT$_7$ heterodimerization specifically attenuates the ability of 5-HT$_{1A}$ receptor to activate G_i protein.

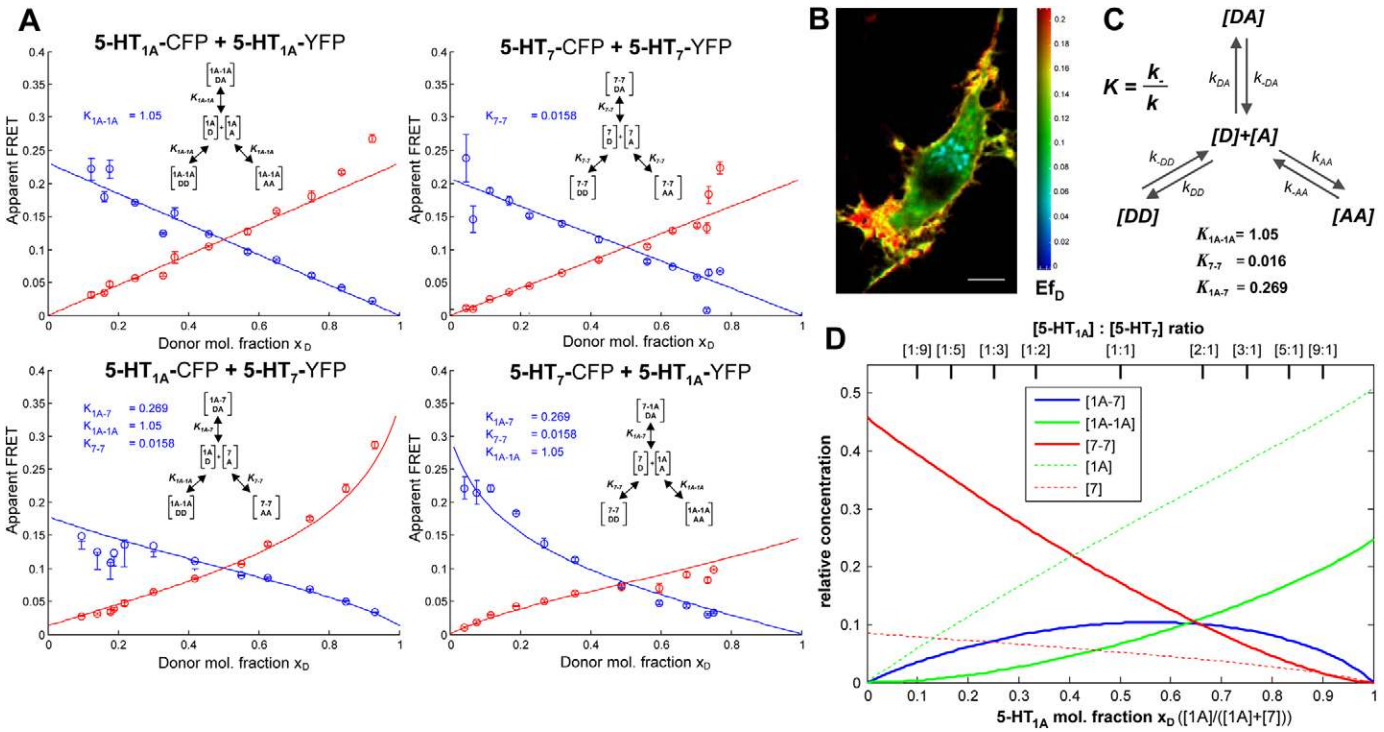

Fig. 3. Dimerization of 5-HT$_{1A}$ and 5-HT$_7$ receptors investigated by lux-FRET. (**A**) Apparent FRET efficiencies Ef_D (blue) and Ef_A (red) were calculated according to a published method (Wlodarczyk et al., 2008) and are shown as functions of the donor mole fraction x_D for homomers of 5-HT$_{1A}$ and 5-HT$_7$ receptors as well as for 5-HT$_{1A}$–5-HT$_7$ heteromers. Experimental data were fitted according to our model for dynamic oligomerization to calculate the following dissociation constants: $K_{5\text{-}HT1A\text{–}5\text{-}HT1A}$=1.05, $K_{5\text{-}HT7\text{–}5\text{-}HT1A}$=0.27 and $K_{5\text{-}HT7\text{–}5\text{-}HT7}$=0.016. Data points represent the mean ± s.e.m. of the apparent FRET efficiency values from three independent experiments. (**B**) Images of apparent FRET efficiency Ef_D in an N1E cell coexpressing 5-HT$_{1A}$–CFP and 5-HT$_7$–YFP receptors were created according to the two-excitation FRET method after confocal microscopy (Woehler et al., 2009). (**C**) Schematic representation of the dimerization model (see Materials and Methods for details). (**D**) Relative concentrations of 5-HT$_{1A}$ and 5-HT$_7$ homodimers (green and red solid lines), 5-HT$_{1A}$–5-HT$_7$ heterodimers (blue solid line) as well as of 5-HT$_{1A}$ and 5-HT$_7$ monomers (green and red dashed lines) were calculated from values of dissociation constants and are shown as function of the donor mole fraction x_D. The total concentration of receptors was assumed to be 1.

The 5-HT$_{1A}$ receptor can also activate the MAP kinases Erk1 and Erk2 (Della Rocca et al., 1999; Papoucheva et al., 2004). We, therefore, next examined whether heterodimerization can influence the Erk phosphorylation in cells expressing a constant amount of 5-HT$_{1A}$ receptors, either alone or together with increased concentrations of YFP-tagged 5-HT$_7$ receptors (Fig. 6B). As shown in Fig. 6C,D, serotonin treatment resulted in a robust increase of Erk phosphorylation in cells expressing 5-HT$_{1A}$ alone, and this response was continuously enhanced after coexpression of increasing amounts of the 5-HT$_7$ receptors. It is noteworthy that increased Erk phosphorylation was not mediated by the co-activation of Erk via the 5-HT$_7$ receptor, because (similarly to the untransfected cells) we did not detect any serotonin-mediated Erk activation in cells expressing the 5-HT$_7$ receptor alone (Fig. 6D). Taken together, these results demonstrate that the degree of heterodimerization specifically regulates 5-HT$_{1A}$-receptor-mediated Erk signalling.

Heterodimerization reduces the ability of 5-HT$_{1A}$ receptor to activate potassium channels in oocytes

G-protein-gated inwardly rectifying potassium (GIRK or Kir3) channels constitute an important physiological downstream target of the 5-HT$_{1A}$ receptor, and channels of this type are activated by direct binding of βγ-subunits of inhibitory G proteins (Huang et al., 1995). Therefore, we next analysed whether the heterodimerization can alter the 5-HT$_{1A}$-receptor-mediated activation of Kir3.1/3.2 concatemers after their coexpression in *Xenopus* oocytes. When 5-HT$_{1A}$ receptors were expressed together with Kir3.1/3.2, basal inward currents of 1.45±0.14 μA (n=23) were elicited upon elevation of the extracellular potassium concentration. Application of 500 nM serotonin further increased current amplitudes to 2.81±0.21 μA (n=23) (Fig. 7A,B). Notably, 5-HT$_7$ receptor expressed together with Kir3.1/3.2 (but without 5-HT$_{1A}$ receptor) did not influence Kir3.1/3.2 channel-mediated currents under basal conditions nor after treatment with serotonin (Fig. 7A, lower trace). However, when 5-HT$_7$ receptors were expressed in addition to 5-HT$_{1A}$ receptors and Kir3.1/3.2, both basal and agonist-induced currents were significantly reduced (basal Kir3.1/3.2 currents decreased to 0.53±0.08 μA and serotonin-mediated current to 0.81±0.11 μA, n=29, P<0.01; Fig. 7A,B). These effects were not mediated by the decreased amount of the 5-HT$_{1A}$ receptor at the cell surface, because receptor density was not altered in oocytes coexpressing 5-HT$_{1A}$ and 5-HT$_7$ receptors (supplementary material Fig. S4A,B). Note that the relative increase in concentrations of injected 5-HT$_7$ receptor RNA led to an increased inhibition of Kir3.1/3.2 currents. Although at a 5-HT$_{1A}$ to 5-HT$_7$ ratio of 1:1 the current amplitude was reduced by 49%, a relative increase in the amount of 5-HT$_7$ cRNA resulting in a ratio of 1:5 led to an augmented reduction of current by 71% (Fig. 7C). The inhibitory

effect of 5-HT$_7$ receptor was not affected after pre-incubation of oocytes with the selective 5-HT$_7$ antagonist SB-269970 (10 μM; Fig. 7D), suggesting the importance of receptor–receptor interaction rather than 5-HT$_7$-receptor-mediated signalling for the Kir3.1/3.2 inhibition.

Finally, we tested whether the inhibitory effect on potassium currents is selectively caused by the coexpressed 5-HT$_7$ receptors or it can be adjusted by other GPCRs. Agonist-induced currents were not significantly changed in comparison with values obtained in oocytes expressing only 5-HT$_{1A}$ receptors when the serotonin receptor 5-HT$_{2C}$ was coexpressed with 5-HT$_{1A}$ (relative current 0.92±0.05, n=5). Also, coexpression of G_s-coupled β1-adrenergic receptors (relative current 0.78±0.15, n=7) as well as G_q-coupled histamine H1 (relative current 0.88±0.11, n=4) or bradykinin B1 receptors (relative current 1.07±0.08, n=7), did not result in any significant change in potassium current (supplementary material Fig. S4C,D). These experiments demonstrate that 5-HT$_7$ receptors can selectively inhibit activation of Kir3.1/3.2 currents via interaction with 5-HT$_{1A}$ receptors.

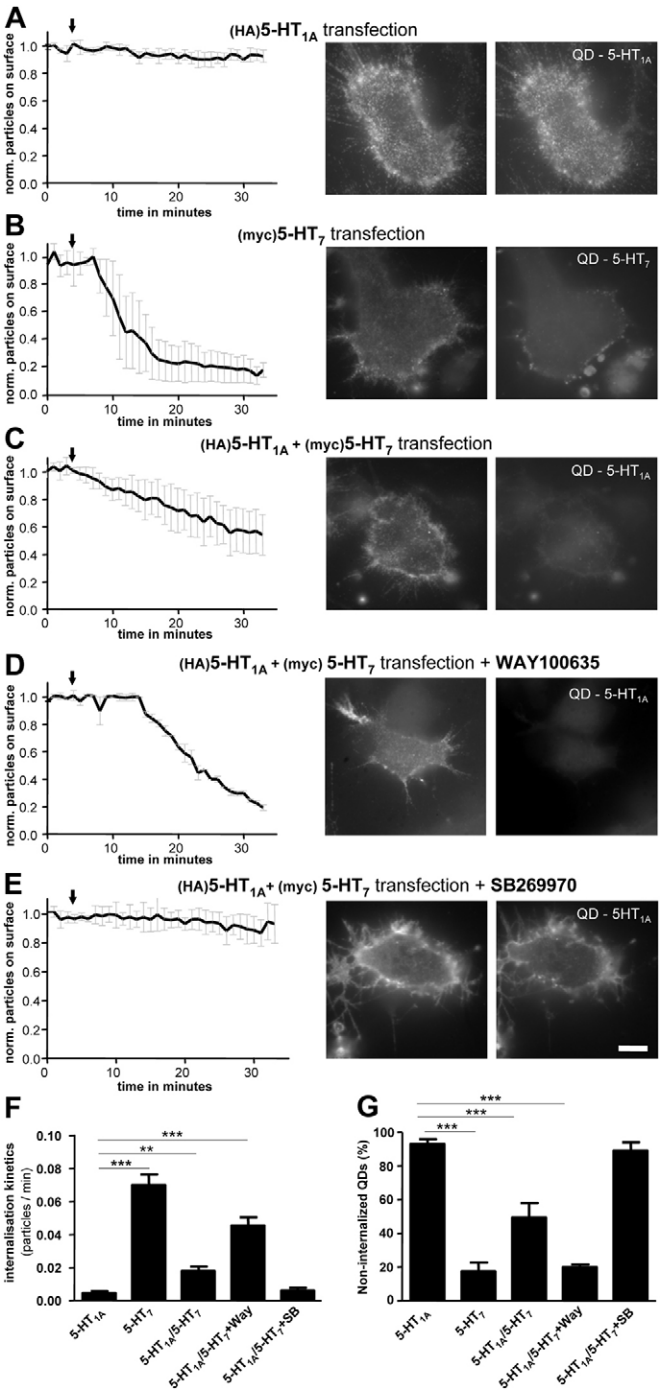

Heterodimerization reduces the ability of endogenous 5-HT$_{1A}$ receptor to activate potassium channels in neurons

Having demonstrated the inhibitory role of 5-HT$_{1A}$–5-HT$_7$ receptor heterodimerization on 5-HT$_{1A}$-receptor-mediated potassium currents in a recombinant system, we next analysed whether this effect also takes place in neurons. As a model system we used mouse hippocampal neurons, which have been shown to produce robust 5-HT$_{1A}$-receptor-mediated K^+ current via GIRK channels (Delling et al., 2002). As illustrated in Fig. 8A, hippocampal neurons express both 5-HT$_{1A}$ and 5-HT$_7$ receptors and these receptors are highly co-localized at the plasma membrane. Co-immunoprecipitation assays performed with brain samples prepared from mice at postnatal day 6 (P6) also demonstrated that these receptor can form heterodimers in vivo (Fig. 8B). To study the functional implication of 5-HT$_{1A}$–5-HT$_7$ heterodimerization, we developed short interfering RNAs (siRNAs) to specifically knockdown the endogenously expressed 5-HT$_7$ receptor (Kobe et al., 2012) (supplementary material Fig. S5A). The expression vectors encoding the specific siRNA also contained GFP, allowing for simple identification of transfected neurons by green fluorescence (Fig. 8C). Transfection of hippocampal neurons with a mixture of 5-HT$_7$ receptor silencing vectors resulted in an increase in basal GIRK currents, as compared with control neurons transfected with the scrambled siRNA (P<0.05, U-test; Fig. 8D,E). Application of 5-HT$_{1A}$ receptor agonist 8-OH-DPAT significantly potentiated GIRK currents in both transfected groups (P<0.05, Wilcoxon

Fig. 4. Heterodimerization promotes agonist-mediated internalization of the 5-HT$_{1A}$ receptor. Internalization of 5-HT$_{1A}$ and 5-HT$_7$ receptors was analysed after specific QD labelling followed by the TIRF microscopy. Appearance of QDs at the plasma membrane was monitored over 30 minutes after the stimulation of receptor with 1 μM serotonin. (**A**) Neuroblastoma N1E-115 cells expressing HA-tagged 5-HT$_{1A}$ receptor alone showed no receptor internalization after stimulation with serotonin. (**B**) The myc-tagged 5-HT$_7$ receptor expressed alone was quickly internalized after stimulation with serotonin. (**C**) Coexpression of HA-tagged 5-HT$_{1A}$ with the myc-tagged 5-HT$_7$ receptors led to serotonin-mediated internalization of 5-HT$_{1A}$ receptor (**D**) Treatment of cells coexpressing 5-HT$_{1A}$ and 5-HT$_7$ receptors with the 5-HT$_{1A}$ antagonist WAY100635 (1 μM) did not block the serotonin-mediated internalization of 5-HT$_{1A}$ receptors. (**E**) By contrast, treatment with 5-HT$_7$ receptor antagonist SB269970 (1 μM) blocked 5-HT$_{1A}$ receptor co-internalization. Application of serotonin is shown by the arrows. The images show the first and last time point for the respective experimental condition (see also supplementary material Movies 1–3). (**F**) Analysis of the internalization kinetics by measuring the slope of the graphs. For conditions with no apparent internalization, slope was calculated for the entire run of the experiment. For experimental conditions that showed internalization, the slope was calculated from the point of first apparent onset of internalization. (**G**) Percentage of the QDs remaining at the cell surface after 30 minutes of 5-HT treatment. Bars show mean + s.e.m. (n=4); **P<0.01, ***P<0.001.

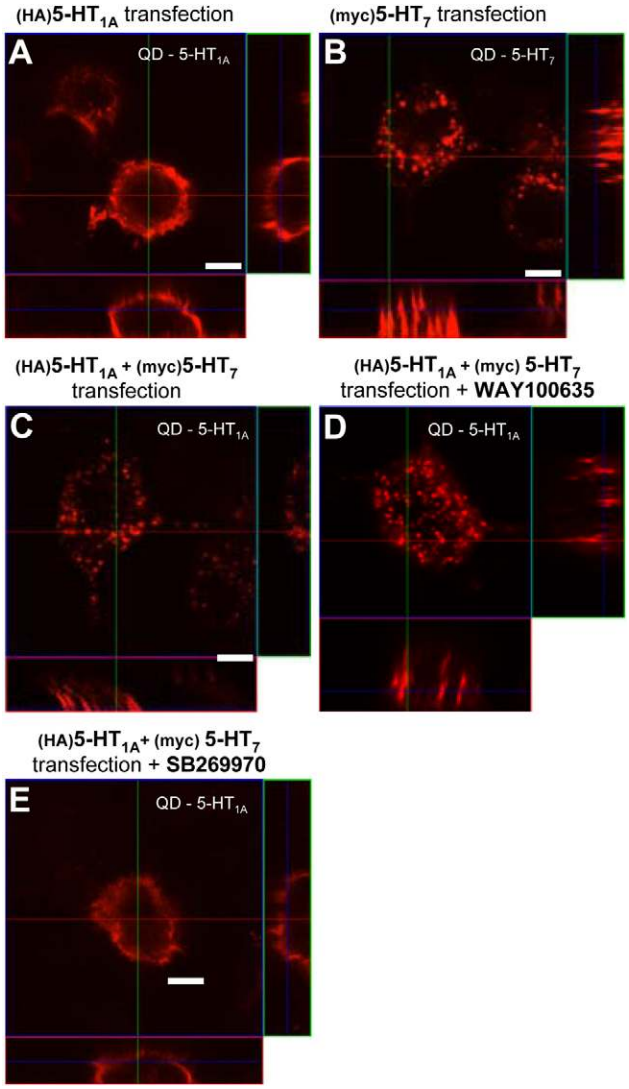

Fig. 5. Analysis of receptor internalization by confocal microscopy. To verify serotonin-mediated internalization of 5-HT_{1A} and 5-HT_7 receptors under the experimental conditions described for Fig. 4, neuroblastoma N1E cells were fixed after TIRF microscopy and subjected to confocal microscopy. Images show orthogonal views of randomly chosen cells. (**A**) In neuroblastoma cells expressing only 5-HT_{1A} receptors, labelled receptors remain at the cell surface after stimulation with serotonin. (**B**) 5-HT_7 receptors are internalized upon serotonin stimulation. (**C**) Co-expression of 5-HT_{1A} and 5-HT_7 receptors leads to internalization of 5-HT_{1A} receptor. (**D**) Treatment of cells coexpressing 5-HT_{1A} and 5-HT_7 receptors with the 5-HT_{1A} receptor antagonist WAY100635 (1 μM) does not block the serotonin-mediated internalization of 5-HT_{1A} receptor. (**E**) Treatment with 5-HT_7 receptor antagonist SB269970 (1 μM) blocks 5-HT_{1A} receptor internalization. Scale bars: 5 μm.

signed rank test), and the amplitude of currents remained significantly larger in 5-HT_7 receptor silenced neurons (Fig. 8D,E). Because all experiments were performed in the presence of 5-HT_7 receptor antagonist SB-269970, these data strongly suggest that direct 5-HT_{1A}–5-HT_7 receptor interaction rather than 5-HT_7-receptor-mediated signalling is responsible for the smaller currents in non-silenced cells.

Finally, we analysed whether the relative concentration of heterodimers, which crucially depends on the expression ratio of both receptors (Fig. 3), undergoes developmental changes. For that, we determined the expression profiles for both 5-HT_{1A} and 5-HT_7 receptors in the mouse hippocampus at different stages of postnatal development using real-time PCR. This approach demonstrated that 5-HT_7 receptor transcripts were strongly expressed during early postnatal stages (P2 and P6) and downregulated during later developmental stages (supplementary material Fig. S5B). By contrast, expression levels of the 5-HT_{1A} receptor mRNA transcripts were not significantly modulated during development (supplementary material Fig. S5C). Because the protein expression level is assumed to roughly correlate with the level of mRNA transcripts, the above data suggest that receptor expression also undergoes developmental regulation. Such differences in the expression levels result in drastic changes of the 5-HT_{1A} to 5-HT_7 ratio from 3:1 at P2, to 6:1 at P6, 12:1 at P12 and 35:1 at P90 (Fig. 8F). According to our dimerization model (Fig. 3D), this means that at the early postnatal stage (P2) hippocampal neurons express similar amounts of homo- and heterodimers ([5-HT_{1A}–5-HT_{1A}]=13% and [5-HT_{1A}–5-HT_7]=9%). During development, the relative concentrations of 5-HT_7 receptors continuously decreased, resulting in a decrease in the amount of 5-HT_{1A}–5-HT_7 heterodimers (e.g. at P90, [5-HT_{1A}–5-HT_{1A}]=23% and [5-HT_{1A}–5-HT_7]=2%). These combined results demonstrate that the relative amount of 5-HT_{1A}–5-HT_7 receptor heterodimers and, consequently, their functional role in inhibition of GIRK currents is progressively decreased during brain development.

Discussion

The existence of GPCR homo- and heterodimers has become generally accepted, and a growing body of evidence points to the functional importance of oligomeric complexes for the receptor trafficking, receptor activation and G protein coupling in native tissues (Bouvier, 2001; Rivero-Müller et al., 2010). The clinical significance of GPCR oligomerization has also become more evident in recent years, leading to identification of receptor oligomers as a novel important therapeutic target (Waldhoer et al., 2005; González-Maeso et al., 2008).

In the present study, we provide biochemical and biophysical evidence for the heteromerization of two serotonin receptors, 5-HT_{1A} and 5-HT_7. Although our experimental results suggest preferential formation of heterodimers, we still cannot exclude the possibility that these receptors can form higher-order oligomers. Indeed, the models that have been previously developed for estimating the number of units interacting in an oligomeric complex can identify a case of dimerization, although they cannot accurately quantify the number of units reacting if this number is above two (Veatch and Stryer, 1977; Meyer et al., 2006). Moreover, homo-FRET analysis of 5-HT_{1A} receptors stably expressed in CHO cells provided first experimental evidence for the existence of higher-order 5-HT_{1A} homo-oligomers (Ganguly et al., 2011). Therefore, future investigations involving homo-FRET experiments in combination with extended oligomerization models will be needed for a better understanding of 5-HT_{1A} and 5-HT_7 oligomerization behaviour.

The results of co-immunoprecipitation experiments in mouse brain provided direct evidence that these receptors can form heteromers in vivo. Utilizing FRET techniques, we demonstrated that 5-HT_{1A} and 5-HT_7 form constitutive and agonist-independent heterodimers at the plasma membrane of living cells. We also found that both 5-HT_{1A} and 5-HT_7 receptors can

form homodimers when expressed alone (Kobe et al., 2008; Woehler et al., 2009). This observation suggests that, in addition to 5-HT$_{1A}$–5-HT$_7$ heterodimers, two types of homodimers composed either of 5-HT$_{1A}$ or 5-HT$_7$ receptors together with the corresponding monomers can simultaneously exist in cells coexpressing both types of receptor (which is often the case in native tissues). This should also be true for other oligomerizing receptors, and the coexistence of the corresponding homomers was experimentally confirmed when heterodimerization of AT$_1$–B$_2$ and δOR–β$_2$AR were analysed (AbdAlla et al., 2000; Jordan et al., 2001). However, the issue of the relative concentration of monomers, homo- and heteromers still remains open, not least because of the absence of suitable methodology. Such knowledge, however, is of particular importance because heterodimers often possess distinct pharmacological or functional properties in comparison with monomers and homodimers (Rozenfeld and Devi, 2011).

So far, various FRET strategies have been used to prove the existence of well-defined complexes only (either homo- or heterodimers). Thus, in the case of heterodimers the possible coexistence and/or quantitative analysis of corresponding homodimer fractions has not been taken into consideration. In the present study, we were able to calculate the relative dissociation constants for hetero- and homodimers by a combination of lux-FRET with an appropriate dimerization model. This model allowed us for the first time to compare the relative concentrations of homo- and heterodimers as well as the corresponding monomers under physiological conditions. A detailed analysis of oligomerization behaviour revealed that the 5-HT$_7$ receptor possesses a higher binding affinity for formation of homodimers than for 5-HT$_7$–5-HT$_{1A}$ receptor heterodimer and 5-HT$_{1A}$ receptor homodimers. One functional consequence of different affinities for homo- and heterodimers is that, even at a relatively low expression level of 5-HT$_7$ receptors, the amount of 5-HT$_7$–5-HT$_{1A}$ receptor heterodimers and, consequently, their functional implication will be relatively high.

Physiological role of heterodimerization during development

Analysis of the functional consequences of dimerization between 5-HT$_{1A}$ and 5-HT$_7$ receptors revealed that heterodimerization decreases the 5-HT$_{1A}$-receptor-mediated activation of G$_i$ protein without affecting 5-HT$_7$-receptor-mediated G$_s$ protein activation. Because G protein activation is mainly mediated through the stabilization of receptor in the active conformation (Gether et al., 2002; Wess et al., 2008), decreased activation of G$_i$ protein in the case of 5-HT$_{1A}$–5-HT$_7$ heterodimer might be explained by the partial destabilization of the 5-HT$_{1A}$ receptor conformation induced by the direct interaction with the 5-HT$_7$ protomer. This might result in formation of a modified binding surface that provides increased specificity for the G$_s$ protein. Based on the atomic model of rhodopsin, it has been proposed that one GPCR

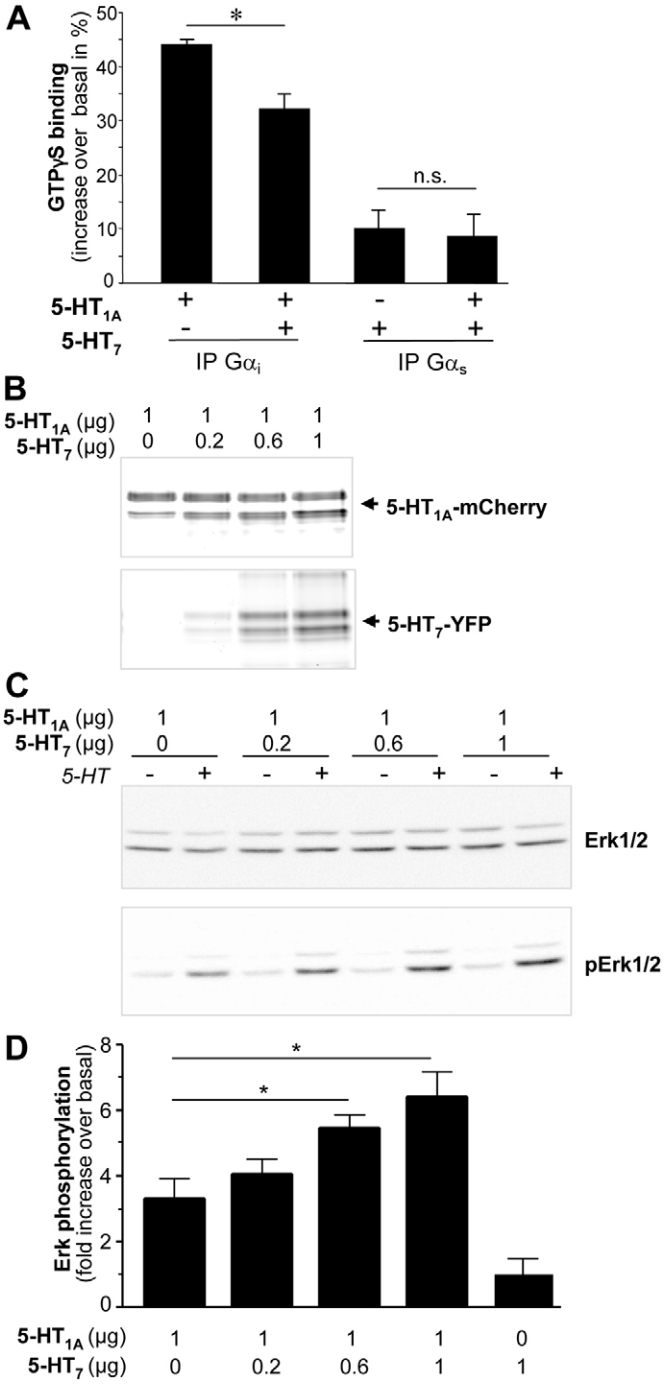

Fig. 6. Heterodimerization alters 5-HT$_{1A}$-receptor-mediated signalling. (**A**) Coupling of the 5-HT$_{1A}$ and 5-HT$_7$ receptors with G$_i$ and G$_s$ proteins, respectively. Membranes were prepared from neuroblastoma cells expressing receptors as indicated and then incubated with [^{35}S]GTPγS in the presence of either vehicle (H$_2$O) or 1 μM serotonin. Immunoprecipitations were performed with appropriate antibodies directed against indicated Gα-subunits. Increase in the [^{35}S]GTPγS binding after serotonin treatment over basal level is shown as a percentage (n=3); *P<0.05; n.s., not significant. (**B–D**) 5-HT$_{1A}$-receptor-mediated Erk activation. Neuroblastoma cells were co-transfected with 1 μg of cDNA encoding for the 5-HT$_{1A}$–mCherry receptor together with increasing concentrations of 5-HT$_7$–YFP receptor and were treated with 10 μM 5-HT or vehicle (H$_2$O) for 5 minutes. (B) Proteins were separated by SDS-PAGE and then subjected to fluorescence imaging to analyse receptor expression. (C) Membranes were probed either with antibodies against the total (upper panel) or phosphorylated (lower panel) Erk. Representative western blots are shown. (D) Quantification of Erk phosphorylation was performed by densitometry and calculated as the ratio of total Erk expression to the Erk phosphorylation signal. Bars show mean + s.e.m. (n=4); *P<0.02.

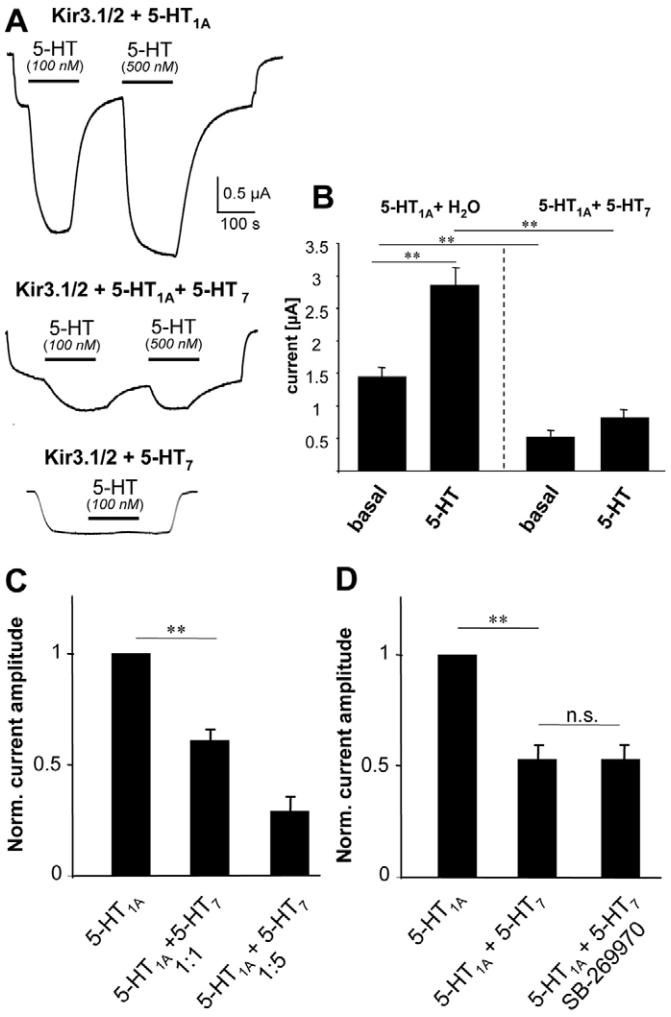

Fig. 7. Heterodimerization decreases 5-HT$_{1A}$-receptor-mediated activation of GIRK channels in oocytes. (**A**) Two-electrode voltage-clamp recordings from oocytes coexpressing Kir3.1/3.2 potassium channels with 5-HT$_{1A}$ and 5-HT$_7$ receptors are shown. Upon elevation of extracellular potassium and application of 5-HT (upper trace) coexpression of 5-HT$_{1A}$ receptors elicits robust inward currents (V_H=−70 mV). Additional co-injection of 5-HT$_7$ receptor RNA results in significant smaller inward currents (middle trace). In the case of coexpression of Kir3.1/3.2 with only 5-HT$_7$ receptors, potassium-mediated basal Kir channel currents are not modulated upon 5-HT application (lower trace). (**B**) Bar graph summarizes basal and 5-HT-induced inward currents of oocytes injected with Kir3.1/3.2 plus either 5-HT$_{1A}$ and H_2O (left) or 5-HT$_{1A}$ and 5-HT$_7$ (right). (**C**) Bar graph representing normalized current amplitudes of 5-HT-induced inward currents after co-injection of 5-HT$_{1A}$ and 5-HT$_7$ at different RNA ratios. (**D**) Normalized current amplitudes of 5-HT-induced inward currents after pharmacological blockage of 5-HT$_7$ receptor with specific antagonist SB-269970 (1 µm). Bars show mean + s.e.m. (n=4); **P<0.01. n.s., not significant.

dimer possesses the optimal docking interface for only one G protein heterotrimer (Fotiadis et al., 2006; Palczewski, 2010). Thus, activation of 5-HT$_7$ protomer in the dimer might induce preferential association of G_s protein with the complex, leading to diminished G_i-protein-mediated signalling. Such mechanism of allosteric modulation between two protomers is further confirmed by the fact that heteromerization often results in an increased G protein activation of the one associated receptor within a heteromer (Rocheville et al., 2000; González-Maeso et al., 2008).

Another important finding in this study is that heterodimerization markedly alters the internalization profile of 5-HT$_{1A}$ receptors. Whereas 5-HT$_{1A}$ receptors expressed alone are resistant to the agonist-mediated internalization, 5-HT$_{1A}$ receptors participating in 5-HT$_{1A}$–5-HT$_7$ heterodimers undergo efficient internalization upon serotonin treatment. The fact that the pharmacological blockade of 5-HT$_7$ receptors, but not of 5-HT$_{1A}$ receptors, abolishes internalization of both 5-HT$_7$ homo- and heterodimers suggests that 5-HT$_7$-receptor-mediated signalling represents an initial step responsible for 5-HT$_{1A}$ co-internalization. Generally, internalization of GPCRs is initiated by the agonist-mediated receptor phosphorylation by GPCR kinases followed by the recruitment of β-arrestin and the assembly of clathrin-coated pits, leading to removal of receptor from the cell surface (Ferguson, 2001; Drake et al., 2006). Once internalized, receptors can initiate additional, G-protein-independent signalling pathways such as a β-arrestin-mediated coupling to MAP kinase (Kovacs et al., 2009). The best-studied example of such signalling is the angiotensin AT$_1$ receptor, which activates MAP kinase Erk in two different ways: first, by a G-protein-dependent pathway that results in transient Erk phosphorylation and targets Erk into the nucleus or, second, by a β-arrestin-dependent pathway that leads to sustained ERK phosphorylation, which directs Erk to the cytosol (Ahn et al., 2004). Such spatio-temporal segregation of ERK signalling has been shown to result in activation of distinct downstream signalling cascades (Luttrell et al., 2001; Wei et al., 2004). Our experimental data suggest that a similar scenario is also relevant for the 5-HT$_{1A}$ receptors residing within 5-HT$_{1A}$–5-HT$_7$ heterodimers. When 5-HT$_{1A}$ receptor monomers and/or homodimers build a dominant population, receptor-mediated G_i protein activation represents the main factor responsible for Erk phosphorylation (Fig. 6) (Papoucheva et al., 2004). In the case of heterodimers, Erk phosphorylation significantly increases (despite the fact that the coupling of 5-HT$_{1A}$ receptor to G_i protein is reduced under these conditions), suggesting that serotonin-mediated co-internalization of 5-HT$_{1A}$ receptor can initiate β-arrestin-mediated Erk phosphorylation. Thus, dependent on the relative amount of heterodimers, this mechanism can allow the same ligand (serotonin) to activate distinct Erk-mediated pathways (i.e. G-protein-dependent or β-arrestin-dependent). This also raises the possibility that conditions that selectively promote or inhibit heterodimerization could have a significant physiological relevance.

In addition, we demonstrated that 5-HT$_{1A}$–5-HT$_7$ heterodimerization markedly decreases the ability of 5-HT$_{1A}$ receptor to activate GIRK channels, an effect mediated through the Gβγ subunits of inhibitory G proteins (Reuveny et al., 1994; Kofuji et al., 1995). The finding that pharmacological blockade of 5-HT$_7$ receptor does not overcome this inhibitory effect suggests that direct receptor–receptor interaction rather than 5-HT$_7$-receptor-mediated signalling is responsible for the reduced GIRK channel activation. The inhibitory effect of 5-HT$_{1A}$–5-HT$_7$ heterodimerization on GIRK channel currents was also found in hippocampal neurons, which suggests a physiological relevance of heteromerization in a neuronal context. The 5-HT$_{1A}$-receptor-mediated opening of GIRK channels, leading to membrane hyperpolarization and a decrease in neuronal input resistance, is one of the main physiological effects of serotonin in the CNS (Araneda and Andrade, 1991; Tanaka and North, 1993; Lüscher et al., 1997).

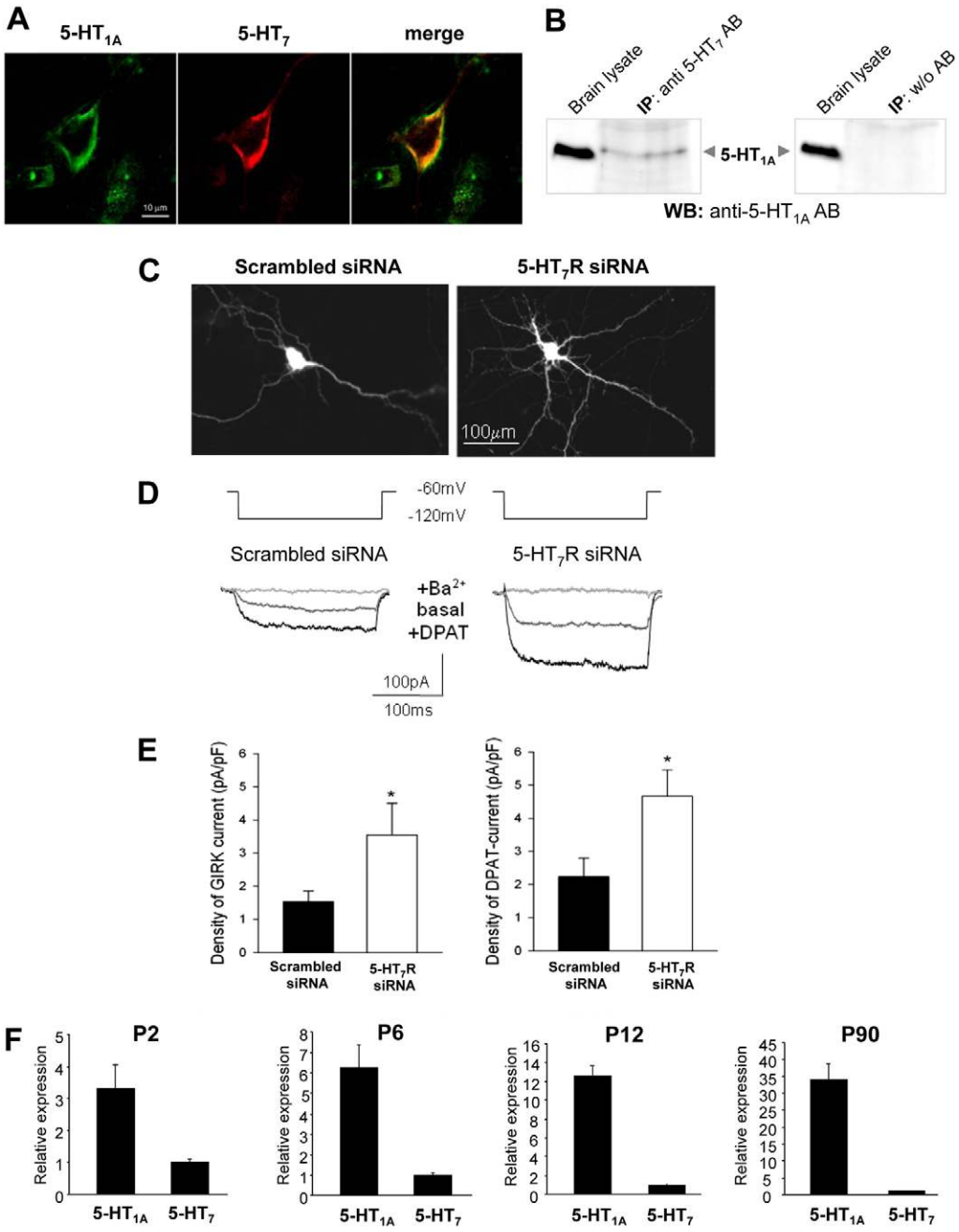

Fig. 8. Heterodimerization decreases GIRK channel currents in hippocampal neurons. (**A**) The 5-HT$_{1A}$ and 5-HT$_7$ receptors are coexpressed in hippocampal neurons. Confocal image of hippocampal neurons at DIV11 is shown. (**B**) Specific co-immunoprecipitation of 5-HT$_{1A}$ and 5-HT$_7$ receptors in samples prepared from the P6 mouse brain. WB, western blot; IP, immunoprecipitation. (**C**) Hippocampal neurons expressing GFP after transfection with control and anti-5-HT$_7$ receptor siRNA plasmids are shown at DIV11. (**D**) Examples of GIRK channel currents in two transfected groups, which showed a strong potentiation after application of 8-OH-DPAT and were fully blocked by $BaCl_2$. (**E**) Summary of recordings from 10 control and 8 siRNA-expressing neurons from three independent culture preparations and transfections. Bars show mean + s.e.m. of the amplitude of basal and 8-OH-DPAT-stimulated GIRK currents; $*P<0.05$ by U-test comparing control and siRNA-expressing neurons. (**F**) Expression ratios between 5-HT$_{1A}$ and 5-HT$_7$ receptors in the mouse hippocampus were determined at different stages of postnatal development using real-time PCR and $\Delta\Delta C_t$ method (see also supplementary material Fig. S5).

With respect to development, it has been shown that the effects of 5-HT on membrane potential undergo pronounced changes. Although at early developmental stages serotonin has only a marginal membrane hyperpolarizing effect, a stronger hyperpolarization becomes the dominant effect of serotonin in adult animals (Segal, 1990; Béïque et al., 2004). Molecular mechanisms underlying such developmental changes in 5-HT action are poorly understood. Our results suggest that differential heterodimerization rates between 5-HT$_{1A}$ and 5-HT$_7$ receptors during development can provide an intriguing explanation for this effect. We found that the expression level of 5-HT$_7$ and 5-HT$_{1A}$ receptors in the hippocampus varies during development. Although the amount of 5-HT$_7$ receptor progressively decreases, the 5-HT$_{1A}$ receptor expression remains relative stable. Therefore, the relative concentration of 5-HT$_{1A}$–5-HT$_7$ heterodimers and, as a consequence, their functional importance also undergo pronounced developmental changes. A relative high expression level of 5-HT$_{1A}$–5-HT$_7$ heterodimers at the early postnatal stages will result in reduced coupling of 5-HT$_{1A}$ receptor to GIRK channels and, consequently, in decreased membrane hyperpolarization due to a lower number of open channels. With increasing age, the relative amount of heterodimers gradually decreases to only 2% at P90, allowing 5-HT$_{1A}$ homodimers together with monomers to become the dominant populations. Thus, the inhibitory influence of heterodimers on basal and 5-HT$_{1A}$-receptor-mediated GIRK channel activation begins to

subside and is gradually replaced by a hyperpolarizing effect mediated by the 5-HT_{1A} homodimers and/or monomers.

Role of heterodimerization in regulation of 5-HT_{1A} receptor internalization

In addition to the role of heterodimerization in regulation of Erk signalling and GIRK channel activation, our results demonstrate that the heterodimerization can modulate the agonist-mediated internalization of 5-HT_{1A} receptor. It has been shown that although the 5-HT_{1A} receptor is expressed both as a presynaptic autoreceptor in serotonergic neurons of raphe nuclei (Hamon et al., 1990; Riad et al., 2000) and as a postsynaptic receptor in multiple brain regions including hippocampus and cortex (Beck et al., 1992; Aznar et al., 2003), chronic receptor stimulation results in functional desensitization of only 5-HT_{1A} autoreceptors without affecting the postsynaptic 5-HT_{1A} receptors (Jolas et al., 1994; Le Poul et al., 1995). Our data suggest that the higher amount of heterodimers produced in presynaptic neurons than in postsynaptic neurons might represent a mechanism responsible for the differential desensitization obtained for the 5-HT_{1A} auto- and heteroreceptors. This is supported by several observations. First, analysis of the brain regional distribution of 5-HT_7 receptor has revealed that this receptor is highly enriched in serotonergic neurons of dorsal raphe nuclei in adults (Neumaier et al., 2001; Bonaventure et al., 2002; Martín-Cora and Pazos, 2004). Together with the finding that the 5-HT_{1A} receptor has a higher affinity for forming heterodimeric (5-HT_{1A}–5-HT_7) rather than homodimeric (5-HT_{1A}–5-HT_{1A}) complexes, this suggests that serotonergic neurons in raphe nuclei express a relative high level of heterodimers, i.e. [5-HT_{1A}–5-HT_7]>[5-HT_{1A}–5-HT_{1A}]. From a functional point of view, this will result in effective co-internalization of 5-HT_{1A} receptor within 5-HT_{1A}–5-HT_7 heterodimeric complexes upon serotonin release.

In the present study, we also found that the expression level of postsynaptic 5-HT_7 receptors in the hippocampus progressively decreased during postnatal development without changes in 5-HT_{1A} receptor expression. Similar results were obtained in forebrain, where expression of 5-HT_7 receptor in pyramidal neurons has been shown to diminish dramatically with increasing age (Béïque et al., 2004). These observations suggest that under physiological conditions 5-HT_{1A} homodimers represent a dominant receptor population in hippocampus in adulthood, i.e. [5-HT_{1A}–5-HT_{1A}]>>[5-HT_{1A}–5-HT_7]. Because 5-HT_{1A} receptors expressed alone are resistant to the agonist-mediated internalization, 5-HT released in hippocampus or cortex will not reduce the amount of postsynaptic 5-HT_{1A} receptors at the cell surface. The mechanism proposed here not only explains the differences in desensitization between pre- and postsynaptic 5-HT_{1A} receptors, but also suggests that the regulated and balanced ratio of homo- and heterodimerization on pre- and postsynaptic neurons might be crucially involved in both the onset and response to treatment of psychiatric diseases such as depression and anxiety.

Materials and Methods

Recombinant DNA procedures, cell culture and transfection

The construction of HA-tagged 5-HT1$_A$ and 5-HT_7 receptors as well as receptors fused to different spectral variants of the green fluorescence proteins has been described previously (Kvachnina et al., 2005; Kobe et al., 2008). YFP-tagged CD86 was a kind gift from Moritz Bünemann, University of Würzburg, Germany (Dorsch et al., 2009). Note that the monomeric versions of CFP and YFP were used to produce all constructs used in the present study. Mouse N1E-115 neuroblastoma cells from the American Type Culture Collection (ATCC) were grown in Dulbecco's modified Eagle's medium (DMEM) containing 10% fetal calf serum (FCS) and 1% penicillin/streptomycin at 37°C under 5% CO_2. For transient transfection, cells were transfected with appropriate vectors using Lipofectamine 2000 (Invitrogen) according to the manufacturer's instructions. The amount of expressed receptor was measured in membrane preparations of transfected cells by using a radioactive ligand binding assay with [^{3}H]8-OH-DPAT as a specific ligand and non-radioactive 5-HT as a competitor.

Co-immunoprecipitation

Co-immunoprecipitation and immunoblotting in neuroblastoma N1E-115 cells coexpressing HA-tagged 5-HT_7 and YFP-tagged 5-HT_{1A} receptors were performed as described (Kobe et al., 2008). The presence of YFP-tagged receptors was verified by the fluorescence scanner Typhoon 9400 (GE Healthcare).

For co-immunoprecipitation analysis from brain, samples from P6 NMRI mice were isolated and homogenized in buffer containing 10 mM HEPES (pH 7.4), 5 mM EGTA, 1 mM EDTA and 0.32 M sucrose. The membrane fraction was then isolated and dissolved in lysis buffer. The lysates were incubated with a rabbit polyclonal antibody directed against the murine 5-HT_7 receptor (1:200 dilution; AbD Serotec, Düsseldorf, Germany) followed by incubation with Protein-A Sepharose, SDS-PAGE and western blot with antibody directed against 5-HT_{1A} receptor (1:200 dilution; Alomone, Jerusalem, Israel). All animal experiments were performed according to the relevant regulatory standards.

Acceptor photobleaching FRET analysis

Images of N1E-115 cells expressing CFP- and YFP-tagged receptors were acquired with an LSM510-Meta confocal microscope (Carl Zeiss Jena) equipped with a 40× 1.3 NA oil-immersion objective at 512×512 pixels. Fluorescence emission was acquired from individual cells over 14 lambda channels, at 10.7-nm steps, ranging from 475 to 625 nm. Linear unmixing was performed by the Zeiss software. Apparent FRET efficiency was calculated offline by the equation:

$$Ef_D = 1 - \left(\frac{F_{DA}}{F_{D'}}\right) \quad (1)$$

where f_D is the fraction of donor participating in the FRET complex (i.e. ratio of concentration of FRET complexes to total donor concentration ($[DA]/[D^t]$), F_{DA} and F_D are the background subtracted and acquisition bleaching corrected pre- and post-bleach CFP fluorescence intensities, respectively. The acquisition bleaching corrected post-bleach CFP intensities were calculated as:

$$F_D = F_D^{B,post} + \left(\frac{F_D^{R,pre} - F_D^{R,post}}{F_D^{R,pre}}\right) F_D^{B,pre} \quad (2)$$

where F_D^B and F_D^R refer to CFP intensities of the bleach and reference region of interest, and *pre* and *post* refer to pre-bleach and post-bleach measurements, respectively.

Spectral FRET analysis in living cells and apparent FRET efficiency calculations

Neuroblastoma N1E-115 cells expressing 5-HT_{1A}–CFP and/or 5-HT_7–YFP receptor were analysed using a spectrofluorometer (Fluorolog 3-22, Horiba JobinYvon, Unterhaching, Germany).

To determine the apparent FRET efficiency for 5-HT_{1A} homodimers, 5-HT_7 homodimers and 5-HT_{1A}–5-HT_7 heterodimers, we used a recently developed lux-FRET method that has been described in detail (Wlodarczyk et al., 2008). This method allows calculation of the total concentration ratio $[A^t]/[D^t]$ of donor and acceptor, a donor molar fraction $x_D=[D^t]/([D^t]+[A^t])$ as well as the apparent FRET efficiencies Ef_D and Ef_A, where $f_D=[DA]/[D^t]$ and $f_A=[DA]/[A^t]$ are the fractions of donors and acceptors in complexes.

During the time-course experiments, the required two emission spectra for lux-FRET analysis were only obtained at the first and last time point by exciting at 440 nm and 488 nm with 2 nm spectral resolutions for emission and 0.5 second integration time. To achieve an appropriate time resolution, only the 440 nm excitation was applied at the intermediate time points, the second excitation data were approximated from the accompanying measurements at the beginning and the end. Stimulation was carried out using 5-HT (Sigma) at a final concentration of 10 μM after 4 minutes. As reference, the same volume of buffer solution was applied.

In all measurements, the spectral contributions due to light scattering and nonspecific fluorescence of the cells were taken into account by fitting reference spectra of donor and acceptor, the emission spectra of non-transfected cells (background) and the Raman scattering spectra to each spectrum.

Dimerization model system

To define the number of monomers participating in oligomer formation, we applied equations suggested by Veatch and Stryer (Veatch and Stryer, 1977). A simplified interpretation of the equation system (Meyer et al., 2006):

$$Ef_D = E\left(1 - x_D^{n-1}\right) \quad Ef_A = E\left(\frac{x_D}{1-x_D}\right)\left(1 - x_D^{n-1}\right) \tag{3}$$

allows us to determine the oligomerization state, whereby n gives the number of monomers in complex. Applying this model to our data we find $n=2$ for both 5-HT$_{1A}$ and 5-HT$_7$ receptors (supplementary material Fig. S1). By contrast, the fit failed for $n=3$ (supplementary material Fig. S1). The general description of the oligomerization behaviour is more complex. The model (Meyer et. al., 2006) does not deliver the true FRET efficiency E, because it does not take into consideration a monomeric fraction. Moreover, if we allow individual rate constants for the corresponding oligomerization partners, eq. 3 cannot be applied. Therefore, we developed a modified dimerization model, assigning individual binding constants for the different kinds of reactions. The rate equation system is schematically illustrated in Fig. 3C. By analysis of the oligomerization behaviour using FRET we can only observe the equilibrated system and, therefore, cannot obtain direct information regarding the rate constants k_i. Thus, we can only discuss the dissociation constants $K_i = k_{-i}/k_i$, where small K values correspond to a high tendency to form dimers. The equation system is then:

The equation system is then:

$$\begin{aligned} K_{DA} &= \frac{k_{-DA}}{k_{DA}} \Rightarrow [D][A] = K_{DA}[DA] \\ K_{DD} &= \frac{k_{-DD}}{k_{DD}} \Rightarrow [D][D] = K_{DD}[DD] \\ K_{AA} &= \frac{k_{-AA}}{k_{AA}} \Rightarrow [A][A] = K_{AA}[AA] \\ [D^t] &= [D] + [DA] + 2[DD] \\ [A^t] &= [A] + [DA] + 2[AA] \end{aligned} \tag{4}$$

which can be combined to the form:

$$\left(-K_{DD} + \sqrt{K_{DD}^2 + 8K_{DD}([D^t] - [DA])}\right)\left(-K_{AA} + \sqrt{K_{AA}^2 + 8K_{AA}([A^t] - [DA])}\right) = 16K_{DA}[DA] \tag{5}$$

Due to the complexity of that fourth order equation (which cab be solved only analytically), it is difficult to apply these for analysis of experimental data. However, several approximations and special cases can provide us with important information about the dimerization process.

For homodimers with $K_{DA} = K_{DD} = K_{AA}$ we receive the well-known linear dependence of eq. 3 mentioned above.

For small K_i values and *high concentration* or *high affinity* of the reaction partners $[D^t] >> K_{DD}$ and $[A^t] >> K_{AA}$ can be assumed. Thus, eq. 5 can be approximated to $\left(\frac{8}{K_{DD}}([D^t] - f_D[D^t])\right)\left(\frac{8}{K_{AA}}([A^t] - f_D[D^t])\right) \approx \left(\frac{16K_{DA}}{K_{DD} \cdot K_{AA}} f_D[D^t]\right)^2$, which can be simplified to $(1-f_D)([A^t]/[D^t] - f_D) \approx \frac{4K_{DA}^2}{K_{DD} \cdot K_{AA}} f_D^2$, resolving to f_D leads to

$$f_D \approx \frac{1 \pm \sqrt{1 - 4\left(1 - 4K_{DA}^2/(K_{DD} \cdot K_{AA})\right) \cdot x_D(1-x_D)}}{2\left(1 - 4K_{DA}^2/(K_{DD} \cdot K_{AA})\right) \cdot x_D} \tag{6}$$

It is notable, that in the high affinity f_D can be expressed as a function of x_D ($f_D = f(x_D)$). However, eq. S4 is only dependent on the product of the dissociation constants $K_{DA}^2/(K_{DD} \cdot K_{AA})$. Thus, we would expect a symmetric functional dependence for f_D and f_A in the high concentration or high affinity case.

For large K_i and *low concentration* or *low affinity* case, eq. 5 can be rephrased as $\left(1 - \sqrt{1 + 8[D^t]/K_{DD}(1-f_D)}\right)\left(1 - \sqrt{1 + 8[A^t]/K_{AA}(1-f_D)}\right) = 16\frac{K_{DA}}{K_{DD} \cdot K_{AA}} f_D[D^t]$, where the terms on the left side can be developed into a Taylor series assuming $[D^t] << K_{DD}$ and $[A^t] << K_{AA}$. Considering only the first term of the Taylor series, $1 - \sqrt{1+x} = -\frac{x}{2} + \frac{x^2}{8} - \frac{x^3}{16} + \frac{5x^4}{128} + O[x]^5$, eq. 5 simplifies to $(1-f_D)([A^t] - f_D[D^t]) \approx K_{DA} f_D$. Resolving to f_D leads to

$$f_D \approx \frac{\left(1 + K_{DA}^*\right) \pm \sqrt{\left(1 + K_{DA}^*\right)^2 - 4x_D + 4x_D^2}}{2x_D} \tag{7}$$

where $K_{DA}^* = K_{DA}/([D^t] + [A^t])$. Due to the approximation, f_D is a function of only K_{DA}, but not of K_{DD} and K_{AA}.

Application of the dimerization model system

In our experiments we found a linear dependence of $f_D = f(x_D)$ for 5-HT$_{1A}$ and 5-HT$_7$ receptor homodimers, but a significantly nonlinear dependence for the heterodimers (Fig. 3A). Moreover, in the case of heterodimer, the dependencies of f_D and f_A were not symmetric. Thus, on the basis of our model we cannot assume the high affinity case. On the other hand, experimental apparent FRET efficiencies allowed us to assume a comparably high quantity of FRET complexes, which is in conflict with the low affinity case. Thus, we analysed the measured apparent FRET dependencies using a numerical solution of eq. 5.

We found that various combinations of K_i and E can fit the individual dependencies with almost similar fit error. Thus, we analysed the dependencies of the individual K_i according to given E values. Supplementary material Fig. S2A,C shows the functional dependence of individual fits for given E from 0.2 to 1 and supplementary material Fig. S2B,D shows the fit parameters K_i and the relative error of the fit result. In the case of homodimers, the model delivers a constant fit quality for E values above a minimal threshold of $E=24\%$ and $E=22\%$, for 5-HT$_{1A}$ and 5-HT$_7$ homodimers, respectively, where higher E values correspond to higher K values. However, the relation between the K values remains preserved, where the K values for 5-HT$_{1A}$ are slightly higher than for 5-HT$_7$ homodimers. The heterodimer model fit requires a significantly higher minimal FRET efficiency than for 5-HT$_{1A}$ and 5-HT$_7$ homodimers. In contrast to the homodimer model fitting, the E value affects the fit quality in the heterodimer cases. For higher E values, the fit error significantly increases. For complexes of 5-HT$_{1A}$–CFP and 5-HT$_7$–YFP the best fit was obtained for $E=40\%$ and for complexes of 5-HT$_7$–CFP and 5-HT$_{1A}$–YFP the best fit was obtained for $E=32\%$. Finally, we prepared a global fit that allowed individual E values for the different homo- and heterodimers (Fig. 3A). Best fitting results were found for E values slightly higher than proposed above for the individual fits. In this case, $K_{5\text{-}HT1A\text{–}5\text{-}HT1A} > K_{5\text{-}HT7\text{–}5\text{-}HT1A} > K_{5\text{-}HT7\text{–}5\text{-}HT7}$, which is in line with results obtained for homodimers.

Model system simulation

With the information on the relative dissociation constants, we simulated the concentration profile of dimers and monomers according to our model for a total concentration ([Dt]+[At]) ranging from 10^{-2} to 10^2 (supplementary material Fig. S3). The concentration pattern at $\log10([5\text{-HT}_{1A}]_{tot} + [5\text{-HT}_7]_{tot}) = 0$ reflects the situation shown in Fig. 3C. For higher total concentrations, $\log10([5\text{-HT}_{1A}]_{tot} + [5\text{-HT}_7]_{tot}) = 2$, the dimer concentration pattern becomes more symmetrical, which was already predicted from the high concentration or high affinity approximation. At this concentration range, monomer concentrations are very small and the fits do not contain any information about individual affinities (see eq. 8). However, at low total concentrations, $\log10([5\text{-HT}_{1A}]_{tot} + [5\text{-HT}_7]_{tot}) = -2$, the monomeric forms are preferentially present. In this case, the distribution of dimers becomes asymmetric with respect to x_D, and the fits become sensitive to individual affinities. However, at this concentration range the dimer concentration becomes very small compared with the monomer concentration. Consequently, the amplitudes of f_D and f_A are very small and FRET signals cannot be detected. Thus, if we observe an asymmetry in the Ef_D and Ef_A functions, we can suggest that monomers and dimers are expressed at similar concentrations (which allows extraction of information about the individual affinities).

Error calculation

In addition to Ef_D, Ef_A and x_D, we can also calculate the error of each parameter from the unmixing error following the error propagation of the lux-FRET equations. In addition to these statistical errors, a systematic error was observed in the Ef_A values in the range of high x_D caused by the mandatory low acceptor emission, which is superimposed and therefore difficult to separate from the cell background signal. All fittings were performed by weighted least square distance minimization. The goodness of the fit was calculated by using the equation:

$$R^2 = 1 - \sum_i (y_i - f(x_i))^2 \Big/ \sum_i (y_i - \bar{y})^2 \tag{8}$$

where y_i are the obtained apparent FRET parameters, $\bar{y}$ their mean value and $f(x_i)$ is the corresponding fit function.

Quantum dot staining and TIRF microscopy

Recombinant N-terminally HA-tagged 5-HT$_{1A}$ and myc-tagged 5-HT$_7$ receptors (Santa Cruz Biotechnology) were used for labelling of receptors with QDs at the surface of living cells. Cells were incubated with 1 ng of primary antibody diluted in OptiMEM for 5 minutes and then extensively washed with OptiMEM before addition of 1 nM QD–Fab conjugates (Invitrogen) in OptiMEM for 5 minutes. QDs were removed by extensive washing over a period of 10 minutes. All staining and washing steps were performed at room temperature.

The TIRF setup was based on an IX71 microscope (Olympus) equipped with a 60× 1.45 NA Plan Apochromat Olympus objective, an Olympus TIRF condenser and a diode laser emitting at 405 nm (Toptica Photonics, Gräfelfing, Germany). Images were acquired with an Andor iXon camera controlled with Andor iQ

software (Andor, Belfast, Northern Ireland). The acquisition rate was 0.25 Hz and the exposure time was 300 milliseconds. To analyse accumulation of receptors in intracellular organelles, three-dimensional reconstructions were made from confocal 3D stacks acquired with a confocal laser-scanning microscope Meta-LSM 510 (Zeiss, Germany). For data acquisition and analysis of confocal images we used the LSM 510 software. Subsequent imaging procedures were performed using NIH ImageJ (http://rsb.info.nih.gov/ij/).

Assays for [^{35}S]GTPγS binding and Erk2 phosphorylation

Agonist-promoted binding of [^{35}S]guanosine 5-(3-*O*-thio)triphosphate to different G proteins caused by stimulation of 5-HT_{1A} and/or 5-HT_7 receptors was performed as described previously (Ponimaskin et al., 2000).

For Erk phosphorylation assay, neuroblastoma cells were transfected with 5-HT_{1A}–mCherry receptor (1 μg of corresponding plasmid) together with increasing amount of 5-HT_7–YFP receptor (0, 0.2, 0.6 and 1 μg of corresponding plasmid). At 24 hours after transfection, cells were stimulated for 5 minutes with 10 μM 5-HT and then lysed in the loading buffer. Equal amounts of proteins in lysates were separated by SDS-PAGE and then subjected to western blot. The membranes were probed either with antibodies raised against phosphorylated Erk1/2 (phospho-p42/44; 1:2000 dilution) or against total Erk (p42/44; 1:1000 dilution). Receptor expression in gels after SDS-PAGE was visualized by the fluorescence scanner Typhoon 9400 (GE Healthcare). The amounts of phosphorylated and total Erk1/2 were quantified by densitometric measurements using GelPro Analyser version 3.1 software.

Injections and electrophysiological analysis in oocytes

For recombinant protein expression in *Xenopus* oocytes, cDNAs of 5-HT_{1A} receptor, 5-HT_7 receptor, 5-HT_{2C} receptor, β1-adrenoreceptors, H1 histamine receptors, B1 bradykinine receptors and Kir3.1/3.2 concatemers were subcloned into the polyadenylation vector pSGEM, respectively. Capped run-off poly(A)+cRNA transcripts were synthesized from linearized cDNA and subsequently injected into defolliculated oocytes. *Xenopus* oocytes were incubated at 20°C in ND96 solution (96 mM NaCl, 2 mM KCl, 1 mM $MgCl_2$, 1 mM $CaCl_2$ and 5 mM HEPES, pH 7.4) supplemented with 100 μg/ml gentamicin and 2.5 mM sodium pyruvate. Two-electrode voltage-clamp recordings were performed 48 hours after injection. Currents were recorded with a Turbo Tec-10 amplifier (npi electronic, Tamm, Germany) and sampled through an EPC9 (HEKA Elektronik, Lambrecht, Germany) interface using Pulse/Pulsefit software (HEKA Elektronik). For rapid exchange of external solution, oocytes were placed in a small perfusion chamber with a constant flow of ND96 or high K^+ medium (96 mM KCl, 2 mM NaCl, 1 mM $MgCl_2$, 1 mM $CaCl_2$ and 5 mM HEPES, pH 7.4).

Whole-cell recordings from hippocampal cultures

Primary murine hippocampal neuronal cultures from 1- to 3-day-old C57BL6/J mice pups were prepared as described previously (Dityateva et al., 2003). On day in vitro 8 (DIV 8), primary hippocampal neurons were transfected with a control pSUPER-Mamm-X/scrambled shRNA plasmid (2 μg per well) or were co-transfected with two plasmids encoding shRNA to silence the expression of 5HT_7 receptor. A modification of the calcium phosphate precipitation method was used for transfection (Jiang and Chen, 2006). Neurons were used for electrophysiological recordings 3–4 days after the transfection. Whole-cell recordings from pyramidal neurons were obtained as previously described (Moult et al., 2006). Electrodes with a resistance of 3–4 MOhm were filled with solution (130 mM potassium gluconate, 8 mM NaCl, 4 mM Mg-ATP, 0.3 mM Na-GTP, 0.5 mM EGTA and 10 mM HEPES, pH 7.25). Cells were perfused continuously with HEPES-buffered saline (HBS) of the following composition: 119 mM NaCl, 5 mM KCl, 2 mM $CaCl_2$, 2 mM $MgCl_2$, 25 mM HEPES, 20 mM D-glucose, 0.0005 mM Na^+ channel blocker tetrodotoxin citrate (Tocris) and 0.001 mM 5-HT_7 receptor antagonist SB269970, pH 7.3. Currents were recorded in GFP-expressing neurons with an EPC 10 USB Patch Clamp Amplifier (HEKA Elektronik). Data acquisition and command potentials were controlled by PATCHMASTER software (HEKA Elektronik) and traces were digitalized at 5 kHz and stored for off-line analysis. To activate GIRK channel currents, 200-millisecond voltage steps from −60 to −120 mV were delivered at 10-second intervals, and leak and capacitive transients were digitally subtracted (Delling et al., 2002). Transfected cultures were coded, and recordings were performed without knowing the identity of delivered plasmids. After recording basal GIRK channel currents, 1 μM of 5-HT_{1A} receptor agonist 8-OH-DPAT was applied, followed by 1 mM $BaCl_2$ to block GIRK currents. The currents recorded in the presence of $BaCl_2$ were digitally subtracted from basal and 8-OH-DPAT-activated currents. The mean amplitudes of currents activated 180–200 milliseconds after the beginning of the voltage step were measured and statistically evaluated using non-parametric tests.

Funding

These studies were supported by the Deutsche Forschungsgemeinschaft (DFG) [grant number PO732] and through the Centre of Molecular Physiology of the Brain (CMPB) to E.G.P., D.W.R. and E.N. A.Z. was supported by the Federal Ministry of Education and Research (BMBF) [grant number 0315690D].

Supplementary material available online at
http://jcs.biologists.org/lookup/suppl/doi:10.1242/jcs.101337/-/DC1

References

AbdAlla, S., Lother, H. and Quitterer, U. (2000). AT1-receptor heterodimers show enhanced G-protein activation and altered receptor sequestration. *Nature* **407**, 94-98.

Ahn, S., Shenoy, S. K., Wei, H. and Lefkowitz, R. J. (2004). Differential kinetic and spatial patterns of beta-arrestin and G protein-mediated ERK activation by the angiotensin II receptor. *J. Biol. Chem.* **279**, 35518-35525.

Araneda, R. and Andrade, R. (1991). 5-Hydroxytryptamine2 and 5-hydroxytryptamine 1A receptors mediate opposing responses on membrane excitability in rat association cortex. *Neuroscience* **40**, 399-412.

Aznar, S., Qian, Z., Shah, R., Rahbek, B. and Knudsen, G. M. (2003). The 5-HT1A serotonin receptor is located on calbindin- and parvalbumin-containing neurons in the rat brain. *Brain Res.* **959**, 58-67.

Barnes, N. M. and Sharp, T. (1999). A review of central 5-HT receptors and their function. *Neuropharmacology* **38**, 1083-1152.

Beck, S. G., Choi, K. C. and List, T. J. (1992). Comparison of 5-hydroxytryptamine1A-mediated hyperpolarization in CA1 and CA3 hippocampal pyramidal cells. *J. Pharmacol. Exp. Ther.* **263**, 350-359.

Béïque, J. C., Campbell, B., Perring, P., Hamblin, M. W., Walker, P., Mladenovic, L. and Andrade, R. (2004). Serotonergic regulation of membrane potential in developing rat prefrontal cortex: coordinated expression of 5-hydroxytryptamine (5-HT)1A, 5-HT2A, and 5-HT7 receptors. *J. Neurosci.* **24**, 4807-4817.

Bonaventure, P., Nepomuceno, D., Kwok, A., Chai, W., Langlois, X., Hen, R., Stark, K., Carruthers, N. and Lovenberg, T. W. (2002). Reconsideration of 5-hydroxytryptamine (5-HT)(7) receptor distribution using [(3)H]5-carboxamidotryptamine and [(3)H]8-hydroxy-2-(di-n-propylamino)tetraline: analysis in brain of 5-HT(1A) knockout and 5-HT(1A/1B) double-knockout mice. *J. Pharmacol. Exp. Ther.* **302**, 240-248.

Bouvier, M. (2001). Oligomerization of G-protein-coupled transmitter receptors. *Nat. Rev. Neurosci.* **2**, 274-286.

Bulenger, S., Marullo, S. and Bouvier, M. (2005). Emerging role of homo- and heterodimerization in G-protein-coupled receptor biosynthesis and maturation. *Trends Pharmacol. Sci.* **26**, 131-137.

Della Rocca, G. J., Mukhin, Y. V., Garnovskaya, M. N., Daaka, Y., Clark, G. J., Luttrell, L. M., Lefkowitz, R. J. and Raymond, J. R. (1999). Serotonin 5-HT1A receptor-mediated Erk activation requires calcium/calmodulin-dependent receptor endocytosis. *J. Biol. Chem.* **274**, 4749-4753.

Delling, M., Wischmeyer, E., Dityatev, A., Sytnyk, V., Veh, R. W., Karschin, A. and Schachner, M. (2002). The neural cell adhesion molecule regulates cell-surface delivery of G-protein-activated inwardly rectifying potassium channels via lipid rafts. *J. Neurosci.* **22**, 7154-7164.

Devi, L. A. (2001). Heterodimerization of G-protein-coupled receptors: pharmacology, signaling and trafficking. *Trends Pharmacol. Sci.* **22**, 532-537.

Dityateva, G., Hammond, M., Thiel, C., Ruonala, M. O., Delling, M., Siebenkotten, G., Nix, M. and Dityatev, A. (2003). Rapid and efficient electroporation-based gene transfer into primary dissociated neurons. *J. Neurosci. Methods* **130**, 65-73.

Dorsch, S., Klotz, K. N., Engelhardt, S., Lohse, M. J. and Bünemann, M. (2009). Analysis of receptor oligomerization by FRAP microscopy. *Nat. Methods* **6**, 225-230.

Drake, M. T., Shenoy, S. K. and Lefkowitz, R. J. (2006). Trafficking of G protein-coupled receptors. *Circ. Res.* **99**, 570-582.

Duncan, M. J., Short, J. and Wheeler, D. L. (1999). Comparison of the effects of aging on 5-HT7 and 5-HT1A receptors in discrete regions of the circadian timing system in hamsters. *Brain Res.* **829**, 39-45.

Fargin, A., Raymond, J. R., Regan, J. W., Cotecchia, S., Lefkowitz, R. J. and Caron, M. G. (1989). Effector coupling mechanisms of the cloned 5-HT1A receptor. *J. Biol. Chem.* **264**, 14848-14852.

Ferguson, S. S. (2001). Evolving concepts in G protein-coupled receptor endocytosis: the role in receptor desensitization and signaling. *Pharmacol. Rev.* **53**, 1-24.

Fotiadis, D., Jastrzebska, B., Philippsen, A., Müller, D. J., Palczewski, K. and Engel, A. (2006). Structure of the rhodopsin dimer: a working model for G-protein-coupled receptors. *Curr. Opin. Struct. Biol.* **16**, 252-259.

Franco, R. (2009). G-protein-coupled receptor heteromers or how neurons can display differently flavoured patterns in response to the same neurotransmitter. *Br. J. Pharmacol.* **158**, 23-31.

Fuxe, K., Ferré, S., Canals, M., Torvinen, M., Terasmaa, A., Marcellino, D., Goldberg, S. R., Staines, W., Jacobsen, K. X., Lluis, C. et al. (2005). Adenosine A2A and dopamine D2 heteromeric receptor complexes and their function. *J. Mol. Neurosci.* **26**, 209-220.

Ganguly, S., Clayton, A. H. and Chattopadhyay, A. (2011). Organization of higher-order oligomers of the serotonin$_1$(A) receptor explored utilizing homo-FRET in live cells. *Biophys. J.* **100**, 361-368.

Garnovskaya, M. N., van Biesen, T., Hawe, B., Casañas Ramos, S., Lefkowitz, R. J. and Raymond, J. R. (1996). Ras-dependent activation of fibroblast mitogen-activated protein kinase by 5-HT1A receptor via a G protein beta gamma-subunit-initiated pathway. *Biochemistry* **35**, 13716-13722.

Gether, U., Asmar, F., Meinild, A. K. and Rasmussen, S. G. (2002). Structural basis for activation of G-protein-coupled receptors. *Pharmacol. Toxicol.* **91**, 304-312.

Gomes, I., Jordan, B. A., Gupta, A., Trapaidze, N., Nagy, V. and Devi, L. A. (2000). Heterodimerization of mu and delta opioid receptors: A role in opiate synergy. *J. Neurosci.* **20**, RC110.

González-Maeso, J., Ang, R. L., Yuen, T., Chan, P., Weisstaub, N. V., López-Giménez, J. F., Zhou, M., Okawa, Y., Callado, L. F., Milligan, G. et al. (2008). Identification of a serotonin/glutamate receptor complex implicated in psychosis. *Nature* **452**, 93-97.

Gordon, J. A. and Hen, R. (2004). The serotonergic system and anxiety. *Neuromolecular Med.* **5**, 27.

Hamon, M., Gozlan, H., el Mestikawy, S., Emerit, M. B., Bolaños, F. and Schechter, L. (1990). The central 5-HT1A receptors: pharmacological, biochemical, functional, and regulatory properties. *Ann. N. Y. Acad. Sci.* **600**, 114-129, discussion 129-131.

Hedlund, P. B. (2009). The 5-HT7 receptor and disorders of the nervous system: an overview. *Psychopharmacology (Berl.)* **206**, 345-354.

Hedlund, P. B. and Sutcliffe, J. G. (2004). Functional, molecular and pharmacological advances in 5-HT7 receptor research. *Trends Pharmacol. Sci.* **25**, 481-486.

Hornigold, D. C., Mistry, R., Raymond, P. D., Blank, J. L. and Challiss, R. A. (2003). Evidence for cross-talk between M2 and M3 muscarinic acetylcholine receptors in the regulation of second messenger and extracellular signal-regulated kinase signalling pathways in Chinese hamster ovary cells. *Br. J. Pharmacol.* **138**, 1340-1350.

Hoyer, D., Pazos, A., Probst, A. and Palacios, J. M. (1986). Serotonin receptors in the human brain. I. Characterization and autoradiographic localization of 5-HT1A recognition sites. Apparent absence of 5-HT1B recognition sites. *Brain Res.* **376**, 85-96.

Huang, C. L., Slesinger, P. A., Casey, P. J., Jan, Y. N. and Jan, L. Y. (1995). Evidence that direct binding of G beta gamma to the GIRK1 G protein-gated inwardly rectifying K^+ channel is important for channel activation. *Neuron* **15**, 1133-1143.

Israilova, M., Tanaka, T., Suzuki, F., Morishima, S. and Muramatsu, I. (2004). Pharmacological characterization and cross talk of alpha1a- and alpha1b-adrenoceptors coexpressed in human embryonic kidney 293 cells. *J. Pharmacol. Exp. Ther.* **309**, 259-266.

James, J. R., Oliveira, M. I., Carmo, A. M., Iaboni, A. and Davis, S. J. (2006). A rigorous experimental framework for detecting protein oligomerization using bioluminescence resonance energy transfer. *Nat. Methods* **3**, 1001-1006.

Jiang, M. and Chen, G. (2006). High Ca^{2+}-phosphate transfection efficiency in low-density neuronal cultures. *Nat. Protoc.* **1**, 695-700.

Jolas, T., Haj-Dahmane, S., Kidd, E. J., Langlois, X., Lanfumey, L., Fattaccini, C. M., Vantalon, V., Laporte, A. M., Adrien, J., Gozlan, H. et al. (1994). Central pre- and postsynaptic 5-HT1A receptors in rats treated chronically with a novel antidepressant, cericlamine. *J. Pharmacol. Exp. Ther.* **268**, 1432-1443.

Jordan, B. A., Trapaidze, N., Gomes, I., Nivarthi, R. and Devi, L. A. (2001). Oligomerization of opioid receptors with beta 2-adrenergic receptors: a role in trafficking and mitogen-activated protein kinase activation. *Proc. Natl. Acad. Sci. USA* **98**, 343-348.

Jordan, B. A., Gomes, I., Rios, C., Filipovska, J. and Devi, L. A. (2003). Functional interactions between mu opioid and alpha 2A-adrenergic receptors. *Mol. Pharmacol.* **64**, 1317-1324.

Kobe, F., Renner, U., Woehler, A., Wlodarczyk, J., Papusheva, E., Bao, G., Zeug, A., Richter, D. W., Neher, E. and Ponimaskin, E. (2008). Stimulation- and palmitoylation-dependent changes in oligomeric conformation of serotonin 5-HT1A receptors. *Biochim. Biophys. Acta* **1783**, 1503-1516.

Kobe, F., Guseva, D., Jensen, T. P., Wirth, A., Renner, U., Hess, D., Müller, M., Medrihan, L., Zhang, W., Zhang, M. et al. (2012). 5-HT$_7$R/G$_{12}$ signaling regulates neuronal morphology and function in an age-dependent manner. *J. Neurosci.* **32**, 2915-2930.

Kofuji, P., Davidson, N. and Lester, H. A. (1995). Evidence that neuronal G-protein-gated inwardly rectifying K+ channels are activated by G beta gamma subunits and function as heteromultimers. *Proc. Natl. Acad. Sci. USA* **92**, 6542-6546.

Kovacs, J. J., Hara, M. R., Davenport, C. L., Kim, J. and Lefkowitz, R. J. (2009). Arrestin development: emerging roles for beta-arrestins in developmental signaling pathways. *Dev. Cell* **17**, 443-458.

Kvachnina, E., Liu, G., Dityatev, A., Renner, U., Dumuis, A., Richter, D. W., Dityateva, G., Schachner, M., Voyno-Yasenetskaya, T. A. and Ponimaskin, E. G. (2005). 5-HT7 receptor is coupled to G alpha subunits of heterotrimeric G12-protein to regulate gene transcription and neuronal morphology. *J. Neurosci.* **25**, 7821-7830.

Le Poul, E., Laaris, N., Doucet, E., Laporte, A. M., Hamon, M. and Lanfumey, L. (1995). Early desensitization of somato-dendritic 5-HT1A autoreceptors in rats treated with fluoxetine or paroxetine. *Naunyn Schmiedebergs Arch. Pharmacol.* **352**, 141-148.

Lee, S. P., So, C. H., Rashid, A. J., Varghese, G., Cheng, R., Lança, A. J., O'Dowd, B. F. and George, S. R. (2004). Dopamine D1 and D2 receptor co-activation generates a novel phospholipase C-mediated calcium signal. *J. Biol. Chem.* **279**, 35671-35678.

Lovenberg, T. W., Baron, B. M., de Lecea, L., Miller, J. D., Prosser, R. A., Rea, M. A., Foye, P. E., Racke, M., Slone, A. L., Siegel, B. W. et al. (1993). A novel adenylyl cyclase-activating serotonin receptor (5-HT7) implicated in the regulation of mammalian circadian rhythms. *Neuron* **11**, 449-458.

Lüscher, C., Jan, L. Y., Stoffel, M., Malenka, R. C. and Nicoll, R. A. (1997). G protein-coupled inwardly rectifying K^+ channels (GIRKs) mediate postsynaptic but not presynaptic transmitter actions in hippocampal neurons. *Neuron* **19**, 687-695.

Luttrell, L. M., Roudabush, F. L., Choy, E. W., Miller, W. E., Field, M. E., Pierce, K. L. and Lefkowitz, R. J. (2001). Activation and targeting of extracellular signal-regulated kinases by beta-arrestin scaffolds. *Proc. Natl. Acad. Sci. USA* **98**, 2449-2454.

Martín-Cora, F. J. and Pazos, A. (2004). Autoradiographic distribution of 5-HT7 receptors in the human brain using [3H]mesulergine: comparison to other mammalian species. *Br. J. Pharmacol.* **141**, 92-104.

Meyer, B. H., Segura, J. M., Martinez, K. L., Hovius, R., George, N., Johnsson, K. and Vogel, H. (2006). FRET imaging reveals that functional neurokinin-1 receptors are monomeric and reside in membrane microdomains of live cells. *Proc. Natl. Acad. Sci. USA* **103**, 2138-2143.

Moult, P. R., Gladding, C. M., Sanderson, T. M., Fitzjohn, S. M., Bashir, Z. I., Molnar, E. and Collingridge, G. L. (2006). Tyrosine phosphatases regulate AMPA receptor trafficking during metabotropic glutamate receptor-mediated long-term depression. *J. Neurosci.* **26**, 2544-2554.

Neumaier, J. F., Sexton, T. J., Yracheta, J., Diaz, A. M. and Brownfield, M. (2001). Localization of 5-HT(7) receptors in rat brain by immunocytochemistry, in situ hybridization, and agonist stimulated cFos expression. *J. Chem. Neuroanat.* **21**, 63-73.

Norum, J. H., Hart, K. and Levy, F. O. (2003). Ras-dependent ERK activation by the human G(s)-coupled serotonin receptors 5-HT4(b) and 5-HT7(a). *J. Biol. Chem.* **278**, 3098-3104.

Paila, Y. D., Kombrabail, M., Krishnamoorthy, G. and Chattopadhyay, A. (2011). Oligomerization of the serotonin(1A) receptor in live cells: a time-resolved fluorescence anisotropy approach. *J. Phys. Chem. B* **115**, 11439-11447.

Palczewski, K. (2010). Oligomeric forms of G protein-coupled receptors (GPCRs). *Trends Biochem. Sci.* **35**, 595-600.

Papoucheva, E., Dumuis, A., Sebben, M., Richter, D. W. and Ponimaskin, E. G. (2004). The 5-hydroxytryptamine(1A) receptor is stably palmitoylated, and acylation is critical for communication of receptor with Gi protein. *J. Biol. Chem.* **279**, 3280-3291.

Parks, C. L., Robinson, P. S., Sibille, E., Shenk, T. and Toth, M. (1998). Increased anxiety of mice lacking the serotonin1A receptor. *Proc. Natl. Acad. Sci. USA* **95**, 10734-10739.

Pazos, A. and Palacios, J. M. (1985). Quantitative autoradiographic mapping of serotonin receptors in the rat brain. I. Serotonin-1 receptors. *Brain Res.* **346**, 205-230.

Ponimaskin, E., Behn, H., Adarichev, V., Voyno-Yasenetskaya, T. A., Offermanns, S. and Schmidt, M. F. (2000). Acylation of Galpha(13) is important for its interaction with thrombin receptor, transforming activity and actin stress fiber formation. *FEBS Lett.* **478**, 173-177.

Pucadyil, T. J., Kalipatnapu, S. and Chattopadhyay, A. (2005). The serotonin1A receptor: a representative member of the serotonin receptor family. *Cell. Mol. Neurobiol.* **25**, 553-580.

Raymond, J. R., Mukhin, Y. V., Gettys, T. W. and Garnovskaya, M. N. (1999). The recombinant 5-HT1A receptor: G protein coupling and signalling pathways. *Br. J. Pharmacol.* **127**, 1751-1764.

Reuveny, E., Slesinger, P. A., Inglese, J., Morales, J. M., Iñiguez-Lluhi, J. A., Lefkowitz, R. J., Bourne, H. R., Jan, Y. N. and Jan, L. Y. (1994). Activation of the cloned muscarinic potassium channel by G protein beta gamma subunits. *Nature* **370**, 143-146.

Riad, M., Garcia, S., Watkins, K. C., Jodoin, N., Doucet, E., Langlois, X., el Mestikawy, S., Hamon, M. and Descarries, L. (2000). Somatodendritic localization of 5-HT1A and preterminal axonal localization of 5-HT1B serotonin receptors in adult rat brain. *J. Comp. Neurol.* **417**, 181-194.

Rivero-Müller, A., Chou, Y. Y., Ji, I., Lajic, S., Hanyaloglu, A. C., Jonas, K., Rahman, N., Ji, T. H. and Huhtaniemi, I. (2010). Rescue of defective G protein-coupled receptor function in vivo by intermolecular cooperation. *Proc. Natl. Acad. Sci. USA* **107**, 2319-2324.

Rocheville, M., Lange, D. C., Kumar, U., Patel, S. C., Patel, R. C. and Patel, Y. C. (2000). Receptors for dopamine and somatostatin: formation of hetero-oligomers with enhanced functional activity. *Science* **288**, 154-157.

Rozenfeld, R. and Devi, L. A. (2011). Exploring a role for heteromerization in GPCR signalling specificity. *Biochem. J.* **433**, 11-18.

Segal, M. (1990). Developmental changes in serotonin actions in rat hippocampus. *Brain Res. Dev. Brain Res.* **52**, 247-252.

Tanaka, E. and North, R. A. (1993). Actions of 5-hydroxytryptamine on neurons of the rat cingulate cortex. *J. Neurophysiol.* **69**, 1749-1757.

Veatch, W. and Stryer, L. (1977). The dimeric nature of the gramicidin A transmembrane channel: conductance and fluorescence energy transfer studies of hybrid channels. *J. Mol. Biol.* **113**, 89-102.

Waldhoer, M., Fong, J., Jones, R. M., Lunzer, M. M., Sharma, S. K., Kostenis, E., Portoghese, P. S. and Whistler, J. L. (2005). A heterodimer-selective agonist shows in vivo relevance of G protein-coupled receptor dimers. *Proc. Natl. Acad. Sci. USA* **102**, 9050-9055.

Wei, H., Ahn, S., Barnes, W. G. and Lefkowitz, R. J. (2004). Stable interaction between beta-arrestin 2 and angiotensin type 1A receptor is required for beta-arrestin 2-mediated activation of extracellular signal-regulated kinases 1 and 2. *J. Biol. Chem.* **279**, 48255-48261.

Wess, J., Han, S. J., Kim, S. K., Jacobson, K. A. and Li, J. H. (2008). Conformational changes involved in G-protein-coupled-receptor activation. *Trends Pharmacol. Sci.* **29**, 616-625.

Wlodarczyk, J., Woehler, A., Kobe, F., Ponimaskin, E., Zeug, A. and Neher, E. (2008). Analysis of FRET signals in the presence of free donors and acceptors. *Biophys. J.* **94**, 986-1000.

Woehler, A., Wlodarczyk, J. and Ponimaskin, E. G. (2009). Specific oligomerization of the 5-HT1A receptor in the plasma membrane. *Glycoconj. J.* **26**, 749-756.